



Mass Balances of the Antarctic and Greenland Ice Sheets Monitored from Space

Inès N. Otosaka¹ · Martin Horwath² · Ruth Mottram³ · Sophie Nowicki⁴

Received: 5 September 2022 / Accepted: 15 May 2023 / Published online: 15 June 2023
© The Author(s) 2023

Abstract

Satellite data have revealed that the Greenland and Antarctic Ice Sheets are changing rapidly due to warming air and ocean temperatures. Crucially, Earth Observations can now be used to measure ice sheet mass balance at the continental scale, which can help reduce uncertainties in the ice sheets' past, present, and future contributions to global mean sea level. The launch of satellite missions dedicated to the polar regions led to great progress towards a better assessment of the state of the ice sheets, which, in combination with ice sheet models, have furthered our understanding of the physical processes leading to changes in the ice sheets' properties. There is now a three-decade-long satellite record of Antarctica and Greenland mass changes, and new satellite missions are planned to both continue this record and further develop our observational capabilities, which is critical as the ice sheets remain the most uncertain component of future sea-level rise. In this paper, we review the mechanisms leading to ice sheets' mass changes and describe the state of the art of the satellite techniques used to monitor Greenland's and Antarctica's mass balance, providing an overview of the contributions of Earth Observations to our knowledge of these vast and remote regions.

Keywords Ice sheets · Sea level · Earth Observations · Greenland · Antarctica

✉ Inès N. Otosaka
ines.otosaka@northumbria.ac.uk

¹ Department of Geography and Environmental Sciences, Centre for Polar Observation and Modelling, Northumbria University, Newcastle-Upon-Tyne NE1 8ST, UK

² Institut Für Planetare Geodäsie, Technische Universität Dresden, 01062 Dresden, Germany

³ Research and Development Department, Danish Meteorological Institute, DK-2100, Copenhagen Ø, Denmark

⁴ Department of Geology and RENEW Institute, State University of New York at Buffalo, Buffalo, NY 14260-1350, USA

Article Highlights

- The Greenland and Antarctic Ice Sheets lose and gain mass through their interactions with the atmosphere and oceans
- There is now a three-decade-long record of ice sheet mass changes from satellite observations, showing that Greenland and Antarctica lost 7.6 trillion tonnes of ice between 1992 and 2020
- The availability and abundance of satellite observations collected over the ice sheets supported new developments of ice sheet models; however, the ice sheets remain the most uncertain component of future sea-level rise

1 Introduction

1.1 The Antarctic and Greenland Ice Sheets

The Greenland and Antarctic Ice Sheets are today's last remaining ice sheets since the Last Ice Age (around 12,000 years ago). Thus, they both store crucial information about the past climate and play an essential role in the current climate system. The polar ice sheets covering most of Greenland and Antarctica are part of the cryosphere—which encompasses all areas made of frozen water, including ice sheets, ice shelves, glaciers, sea ice, lake and river ice, permafrost, and snow. Among different elements of the cryosphere, ice sheets and glaciers directly influence global mean sea level by raising sea levels when they lose ice. While mountain glaciers contain less than 1% of the global ice volume (Farinotti et al. 2019), the polar ice sheets cover vast areas and store about 68% of the Earth's freshwater resources. The Greenland Ice Sheet covers an area of 1.7 million km² and stores a volume of 3.0 million km³ of ice (Morlighem et al. 2017), while the Antarctic Ice Sheet covers an area 4 times larger (12.3 million km², excluding the ice shelves) and stores 26.5 million km³ of frozen water (Fretwell et al. 2013). Combined, the two ice sheets hold enough frozen water to raise global mean sea level by 65.3 m, with the Greenland Ice Sheet holding a potential sea-level rise of 7.42 m (Morlighem et al. 2017) and the Antarctic Ice Sheet an equivalent sea-level rise of 57.9 m (Morlighem et al. 2020).

The Antarctic Ice Sheet is centred on the South Pole and is surrounded by the Southern Ocean (Fig. 1a). It is divided into the West and East Antarctic Ice Sheets by the Transantarctic Mountains. West Antarctica is the most vulnerable region of the continent as its bedrock is grounded well below sea level and is therefore at greater risk than other parts of the ice sheet. Indeed, the ice sheet bed in West Antarctica is deeper at its centre than at the grounding line, suggesting that West Antarctica is prone to marine ice sheet instability (Mercer 1978; Schoof 2007). The instability hypothesis has been formulated for parts of the ice sheets where the grounding line—the boundary between the grounded ice and floating ice shelf—is located on an upward sloping bed. In that configuration, a retreat of the grounding line leads to an increase in ice discharge as the ice thickness increases inland and in turn entails a further retreat of the grounding line in a hysteretic behaviour. This unstable retreat goes on until a region with a downward sloping bed or a new pinning point is reached. West Antarctica counts some of the world's fastest glaciers, with the prominent examples of Pine Island and Thwaites Glaciers located in the Amundsen Sea Embayment (Rignot 2008). The Antarctic Peninsula is the northernmost region of Antarctica and is often distinguished from the rest of the West Antarctic Ice Sheet due to its

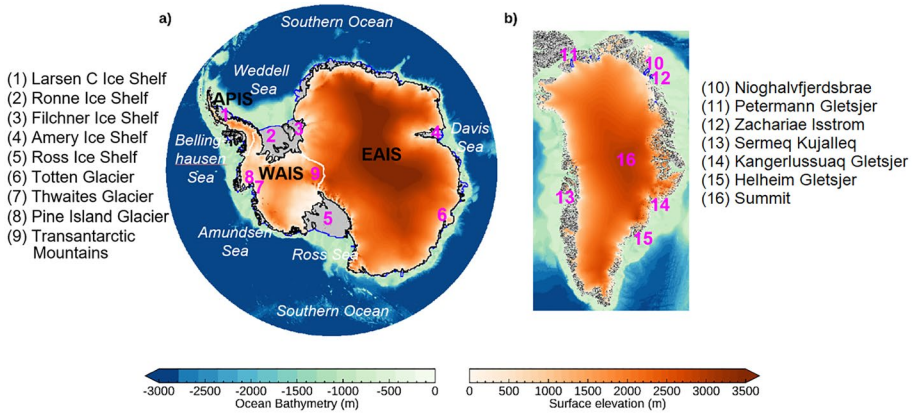


Fig. 1 Surface elevation of the **a** Antarctic and **b** Greenland Ice Sheets and bathymetry of the Southern and Arctic Oceans. Black contours indicate the grounded ice sheet and blue contours indicate ice shelves and floating ice tongues boundaries. White contours indicate the division of West Antarctica (WAIS), East Antarctica (EAIS) and the Antarctic Peninsula (APIS). Surface elevation, and bathymetry data are from the REMA DEM (Howat et al. 2019) and the IBCSO (Arndt et al. 2013) for Antarctica and from the GIMP DEM (Howat et al. 2015) and BedMachine v3 (Morlighem et al. 2017) for Greenland

milder climate. The Antarctic Peninsula is a mountainous region extending over more than 1300 km and has experienced the highest level of warming compared to the rest of the continent (Vaughan et al. 2003). On the other side of the Transantarctic Mountains lies the East Antarctic Ice Sheet, covering about 85% of the Antarctic Ice Sheet. Most of East Antarctica is grounded well above sea level and has not undergone dramatic changes over the past four decades, unlike what has been observed in West Antarctica (Gardner et al. 2018). About 30 major ice streams drain the Antarctic Ice Sheet, transporting about 90% of ice and sediment from the interior to the margins of the ice sheet (Bamber et al. 2000). These ice streams are typically tens of kilometres wide, extend inland up to a thousand of kilometres, and flow at speeds of around 800 m year⁻¹ (Bennett 2003). Finally, the Antarctic Ice Sheet is fringed by ice shelves—covering an area of 1.6 million km² (Fretwell et al. 2013). Ice shelves are platforms of floating ice that are connected to the grounded ice sheet, which play an important role on the stability of the ice sheet by exerting back-stresses on the grounded ice (Dupont and Alley 2005).

In the Northern Hemisphere, the Greenland Ice Sheet is the largest ice-covered land and is about 1000 km wide and 2500 km long (Fig. 1b). Greenland is surrounded by the North Atlantic subpolar gyre, Baffin Bay, the Arctic Ocean, and the Greenland Sea. Greenland counts more than 200 major outlet glaciers. More than half of these glaciers are tidewater in direct contact with the ocean while the remainder are land-terminating glaciers or glaciers ending in ice shelves (Moon et al. 2012) with the largest glaciers of the Greenland Ice Sheet—Helheim Gletsjer, Sermeq Kujalleq (also known as Jakobshavn Isbrae), and Petermann Gletsjer—draining to the ocean. Compared to Antarctica, Greenland’s glaciers are much narrower and extend over a width of a few kilometres at their terminus. Greenland’s outlet glaciers typically flow at a speed of hundreds of meters per year—though a record velocity of 17 000 m year⁻¹ was recorded at Sermeq Kujalleq in summer 2012 (Joughin et al. 2014b)—discharging about ~500 gigatons (Gt) of ice to the ocean ever year (King et al. 2020).

1.2 Ice Sheets in the Earth's System

The ice sheets both influence and are influenced by the components of the Earth's climate system through their interactions with their shared atmosphere and oceans. Through interactions with the atmosphere, the ice sheets gain mass through snowfall accumulation and lose mass through meltwater runoff from surface melting. In response to oceanic forcing, they lose mass at their edges through contact with warm ocean waters and from submarine melting of their floating ice shelves and floating ice tongues. In turn, the ice sheets can affect atmospheric circulation patterns through changes in their topography and ocean circulation patterns as meltwater that runs off from the ice sheet constitutes an input of freshwater to the ocean. In addition to interacting with the climate system, the ice sheets also interact with the solid Earth (Whitehouse et al. 2019). When the ice sheets grow or shrink, the lithosphere beneath deforms in response to this mass change. This viscoelastic response of the solid Earth, or glacial isostatic adjustment (GIA), is translated by an uplift of the surface when the ice sheets shrink and a subsidence of the surface when they grow. This deformation of the solid Earth occurs both over very long time scales—the solid Earth is still adjusting to the last deglaciation which began 21,000 years ago (Peltier 2004)—and shorter time scales (annual to decadal) due to present day mass changes.

These two-way interactions are also at the origin of feedback effects, which can further amplify or dampen signals of imbalance that have been observed in some regions of Antarctica and Greenland (Fyke et al. 2018). One such example is the 'ice-albedo' feedback. The ice sheets, which are covered by snow and ice, have a higher surface reflectivity (albedo) than other surfaces and reflect up to 90% of the incoming solar energy back to space, keeping the Earth cool. However, as the surface of the ice sheets melts, the darker bare ground underneath is exposed, which leads to more solar radiation being absorbed by the ground and also results in further melting of the surrounding snow and ice in a positive feedback loop. This positive feedback loop can be further enhanced by the growth of brown-pigmented algae at the surface of the ice sheets, which results in a darkening of the surface and further reduction in the bare ice albedo (Stibal et al. 2017). On the other hand, for marine ice sheets experiencing a rapid retreat, the bedrock uplift induced by the GIA combined with the sea surface height decreases from reduced gravitation pull of the ice sheet on ocean waters result in a stabilising effect on grounding line retreat (e.g. Gomez et al. 2010; Konrad et al. 2015). This is suspected to be particularly relevant in the Amundsen Sea Sector where rapid mass loss has been observed and where the low mantle viscosity results in rapid uplift rates as a response to the mass loss (Barletta et al. 2018). Modelling the interactions between West Antarctica mass changes and the solid Earth has shown that it could lead to a reduction in Thwaites' grounding line retreat of 38% in 350 years (Larour et al. 2019). There are other examples of feedback mechanisms that would contribute to stabilise or destabilise the ice sheets, and modelling the impact of these feedback mechanisms on the future evolution of the ice sheets under different climate warming scenarios is an active area of ongoing research.

As we have seen, Greenland and Antarctica are integral parts of the climate system, and thus, they are also affected by global warming. Global mean surface temperature is currently rising at a rate of 0.2 °C per decade compared to pre-industrial time due to the anthropogenic increase in greenhouse gas concentrations in the atmosphere. It is estimated that human-induced warming of 1 °C above pre-industrial levels was reached around 2017 (Masson-Delmotte et al. 2018). However, the level of warming is not uniform across the globe and some regions, in particular the Arctic, have experienced a more pronounced

level of warming than the rest of the world, with air temperatures increasing at a rate more than twice that of the global average (Meredith et al. 2019). In the Southern Hemisphere, rapid regional warming has been observed at the Antarctic Peninsula with air temperatures increasing at a rate of 0.3 ± 0.2 °C per decade during the period 1979–1997. However, this region also exhibits extreme natural internal variability in atmospheric circulation as this warming period was followed by a cooling of -0.5 ± 0.3 °C during the period 1999–2014 (Turner et al. 2016). Water from the Bellingshausen and Amundsen seas, intruding the continental shelf, has warmed at a rate of 0.1 to 0.3 °C per decade since the 1990s (Schmidtko et al. 2014). The response of the ice sheets to this changing climate is expected to have wide impacts on sea level, ocean circulation, and ecosystems.

1.3 Consequences of Ice Sheet Mass Loss

When the ice sheets melt, they directly contribute to rising sea levels: adding 360 gigatons of water to the ocean results in an increase in global mean sea level of 1 mm. Between 1992 and 2017, ice losses from Greenland and Antarctica have contributed 17.8 ± 1.8 mm to global mean sea-level rise (Shepherd et al. 2018, 2020). Ice losses from the Greenland and Antarctic Ice Sheets now represent about a quarter of the total sea-level budget, contributing 0.66 mm year⁻¹ and 0.19 mm year⁻¹ to the rate of sea-level rise (3.1 mm year⁻¹) between 2002 and 2017, respectively (Nerem et al. 2018). However, while the values quoted above refer to global mean sea-level rise, it is important to note that input meltwater from the ice sheets to the oceans is redistributed unevenly across the globe due to solid Earth deformation coupled with gravitational effects, in a pattern named as ‘sea-level fingerprint’ (Farrell and Clark 1976). When an ice sheet loses ice, it affects the Earth’s gravitational field by pulling away the nearby ocean waters inducing a sea-level fall in the vicinity of the ice sheet and a sea-level uplift towards faraway coastlines (Hsu and Velicogna 2017). Increase in sea level has direct societal and economic implications. It is estimated that about 110 million people are currently living in low elevation coastal areas below the high tide line, putting them at risk of coastal inundation. It is projected that even under a low carbon emission scenario, a further 80 million would be exposed to coastal flooding if sea-level rise by 30 to 80 cm by 2100 (Kulp and Strauss 2019). To inform governmental policy and plan effective mitigation measures to protect coastal areas, tracking the contribution of the ice sheets to global mean and local sea-level rise is crucial for stakeholders to plan for the future (Shepherd and Nowicki 2017).

The impacts of ice sheets losing mass also have far-reaching impacts on the global climate system. In addition to contributing to global mean sea-level rise, mass loss from the ice sheets constitutes an input of freshwater to the ocean, potentially affecting ocean circulation patterns. In the Northern Hemisphere, meltwater from the Greenland Ice Sheet has been linked to the weakening of the Atlantic meridional overturning circulation (AMOC) (Böning et al. 2016; Caesar et al. 2018). On the other hand, climate simulations of Antarctica’s future ice losses have shown that increased meltwater from Antarctica would lead to a warming of the Southern Ocean subsurface, further enhancing melting at the edge of the ice sheet (Golledge et al. 2019). Finally, additional meltwater input from the ice sheets is predicted to enhance global temperature inter-annual variability up to 50% by 2100, leading to more frequent extreme weather events (Golledge et al. 2019).

2 Ice Sheet Mass Balance

Ice sheets gain mass through snowfall accumulation and lose mass through meltwater runoff caused by surface melting, through ice dynamics processes which result in solid ice discharge across the grounding line of the ice sheets—the boundary between the grounded and floating ice—and subsequent iceberg calving, and through basal melt at the bed of the ice sheets. The sum of these processes is called mass balance. If the mass balance is positive, the ice sheet is gaining mass and if negative, it is losing mass. The mass balance of the ice sheets (MB) is calculated as the difference between the surface mass balance (SMB) and the solid ice discharged across the grounding line of the ice sheets (D), and basal mass balance (BMB):

$$MB = SMB - D - BMB \quad (1)$$

2.1 Surface Mass Balance

Surface mass balance (SMB), sometimes referred to as surface mass budget or climatic mass balance (Cogley et al. 2011), describes the balance between ice gain via accumulation of snow on the one hand and ice loss, known as ablation on the other. Ablation includes ice loss by sublimation, evaporation melt, and runoff (Lenaerts et al. 2019). Glaciers and ice sheets can only gain ice via surface accumulation; all other mass budget terms are negative and include calving and ocean driven melt of outlet glaciers terminating in the ocean, as well as basal melting from floating ice shelves and at the base of glaciers (e.g. Mankoff et al. 2021; Mottram et al. 2019). SMB therefore needs to be strongly positive to keep an ice sheet in balance or growing, as it also needs to balance the dynamic part of the ice budget. Although all glaciers, ice caps, and ice sheets have the same SMB processes, the relative importance of different parts of the SMB calculation can vary widely. In Antarctica, snowfall is by far the most important term with relatively only very small amounts of melt and runoff, apart on ice shelves which can experience significant melt and where the formation of large melt ponds is associated with sudden ice shelf collapse and subsequent acceleration of their tributaries glaciers (Banwell et al. 2013; De Angelis and Skvarca 2003). In Greenland, ablation and melt are much more important and explain a larger proportion of the SMB.

The area of a glacier where more snow falls than melts off over the course of an annual cycle is called the accumulation zone, and the area where more ice is melted than accumulates by snowfall is the ablation zone. In the accumulation zone, the surface becomes compacted by repeated snow falls and is eventually transformed to glacier ice that flows under pressure. In the ablation zone, all the seasonal snow melts off and underlying glacier ice is often exposed also to melt. The line between these two, known as the equilibrium line, is on closer inspection more like a wide zone. Within this percolation zone, there are patches of snow and exposed ice as well as streams and ponds of meltwater. In the upper percolation zone, the annually accumulated seasonal snow melts but does not usually entirely disappear at the end of the melt season. Recently, satellite observations have clearly revealed an expansion of the percolation zone as well as meltwater lakes across Greenland as a result of increasing melt rates (Leeson et al. 2015).

Accumulation by snowfall varies from light diamond dust snowflakes in drier, colder interior regions, where accumulation rates are counted in millimetres per year, to heavy

snowfalls of a few metres per year in typically warmer and wetter coastal regions. Ice sheet accumulation is typically episodic, with a few large cyclonic storms accounting for the majority of the snowfall at both ice sheets. In some locations, particularly in coastal areas, atmospheric rivers may bring several years' worth of annual snowfall over only a few days (e.g. Mattingly et al. 2018; Willen et al. 2021). Ice sheet ablation occurs mostly through melt and runoff but in some regions, most notably the vast dry and windy interior of Antarctica, sublimation and evaporation are also important processes (Agosta et al. 2019). The presence of liquid melt water at the surface can be detected from microwave satellite data, but to calculate the amount of melt requires models based either on output from regional climate and weather models, or from measurements with a weather station. Once melted, liquid water, which may also include rainfall, percolates down into deeper levels in the snow pack and, depending on the "cold content" of the snow pack, refreezes, forming ice lenses that can in some places coalesce to form large ice slabs that may be metres thick and extend over kilometres (MacFerrin et al. 2019). These lenses and slabs form barriers to further percolation and reduce the capacity of the snowpack to absorb further meltwater. If there is a sufficiently thick and warm snowpack, liquid meltwater percolating into deeper layers can remain liquid even through the winter period, filling the pore space inside the snow layers in a so-called firn aquifer.

SMB is measured directly with repeat measurements at stakes drilled into the ice sheet surface (van As et al. 2011) and with the assistance of shallow firn cores in the accumulation zone where annual layers can sometimes be discerned (Machguth et al. 2016; Medley and Thomas 2019). However, these point measurements are difficult to generalise over a wider area without remote sensing techniques such as snow radar or lidar altimetry (Koenig et al. 2016). For this reason, output from climate or weather forecast models is often used to estimate SMB and then in combination with discharge datasets from satellite observations used to assess the total mass budget of ice sheets (e.g. Ettema et al. 2010; Shepherd et al. 2018, 2020). There exist different types of SMB models, including positive degree day models, energy balance models, regional climates models (RCMs), and general circulation models (Fettweis et al., 20,200). RCMs forced by climate reanalyses at their boundaries are most commonly used to estimate the SMB component of the mass budget method as they simulate the transfers of energy between the atmosphere and the surface at high resolution. Examples of RCMs include HIRHAM (Lucas-Pitcher et al. 2012), MAR (Modèle Atmosphérique Régional, Fettweis et al. 2017; Agosta et al. 2019), and RACMO (Regional Atmospheric Climate Model, Noël et al. 2018; van Wessem et al. 2018).

However, differences between models can lead to varying estimates of SMB both in terms of the relative mass of accumulation compared to ablation and in the geographical spread of SMB across an ice sheet (see for example Fettweis et al. 2020 in Greenland; Mottram et al. 2021 in Antarctica). These differences, due to different model resolution, physics, and dynamical schemes, must be taken into consideration when making combined estimates of ice sheet mass budget as they introduce an extra level of uncertainty that also influences ice sheet dynamics in ice sheet models for example. Some models are increasingly using assimilation techniques for Earth Observation data, for example, satellite derived albedo (e.g. Langen et al. 2017) and melt (Mote 2007) to improve calculated SMB. As climate changes, there is also increasing evidence that mean temperature and precipitation changes alone are not sufficient to explain likely ice sheet evolution as atmospheric circulation can have a large influence on both melt and precipitation. Clear sunny skies in summer and/or warm moist air masses moving over ice sheets bring large amounts of melt energy that can be significant on annual to decadal time scales. High

snowfall events associated with cyclonic weather systems and atmospheric rivers can also influence SMB longer time periods, especially given the importance of feedbacks related to surface albedo and the formation of a thick snow pack that can buffer melt rates by refreezing meltwater at depth. This means that for both ice sheets, considering regional scale circulation patterns and weather extremes are as important as average climate when assessing future SMB changes related to climate change.

2.2 Ice Dynamics

Ice sheets flow slowly from their centre towards their margins under their own weight with speed ranging from centimetres per year in the interior to kilometres per year in some of the fastest outlet glaciers and ice streams. Here we define ice dynamics processes as processes that result in a change in ice flow, causing a subsequent change in the rate of solid ice being discharged to the ocean. While SMB processes occur across the whole ice sheets, solid ice is discharged locally through glaciers and ice streams directly to the ocean or to the adjacent floating ice shelves and ice tongues. Ice can be discharged from the ice sheets to the ocean via underwater melting and iceberg calving of marine terminating glaciers (Joughin et al. 2012).

Thinning of ice shelves and tidewater glaciers' floating ice tongues due to melting at the ice-ocean interface leads to ice flow acceleration near the grounding line (Holland et al. 2008), further inducing thinning of the ice upstream (Shepherd et al. 2002) and grounding line retreat (Park et al. 2013). In Antarctica, this phenomenon is particularly important as 75% of Antarctica's coastline is fringed by ice shelves. Ice shelves play a very important role in the dynamic stability of the Antarctic Ice Sheet: by exerting back stress ('buttressing') to the grounded ice upstream, ice shelves hold back the glaciers and contribute to stabilising their grounding lines and ice flux. When ice shelves experience extensive thinning, this can lead to a destabilisation of the grounded ice sheet upstream due to a loss in buttressing to the grounded ice sheet (Dupont and Alley 2005), leading to glaciers sped up and further thinning (Gudmundsson et al. 2019). The intrusion of warm subsurface water close to the edge of marine-terminating glaciers and beneath ice shelves is dependent on the bed topography (Seroussi et al. 2017), and submarine melt rates are highly variable both spatially (Wilson et al. 2017) and temporally over a range of different time scales from weeks to months (Davis et al. 2018). Ice shelves in the Amundsen and Bellingshausen seas have thinned by up to 18% of their thickness in 2012 compared to 1994 (Paolo et al. 2015). Cavities under ice shelves promoting the circulation of Circumpolar Deep Water (CWD) have been identified as a trigger for submarine melting, removing more than 300 m of solid ice beneath Smith Glacier between 2002 and 2009 (Khazendar et al. 2016). Consequently, ice dynamic losses are the greatest in the Amundsen Sea Embayment with a 77% increase in ice discharge between 1973 and 2013 due to the sped up of Pine Island, Thwaites, Pope, Smith, and Kohler glaciers (Mouginot et al. 2014), and ice thinning over these glaciers exceeds 3 m year⁻¹ (Flament and Rémy 2012).

In addition to submarine melting, the polar ice sheets lose mass at the margins of the ice shelves and termini of marine glaciers through iceberg calving, releasing chunks of ice to the ocean (Enderlin et al. 2014). Iceberg calving is initiated by the formation of small cracks on the surface of glaciers and ice shelves, further growing into crevasses, a process that can be enhanced through hydro-fracturing of water-filled crevasses or meltwater undercutting (Benn et al. 2007). Major calving events occurred in

the Antarctic Peninsula over the Larsen A and B ice shelves, leading to their disintegration in 1995 and 2002, respectively. These events induced the speed-up and thinning of the ice shelves' tributary glaciers. Following the collapse of the Larsen B ice shelf in the Antarctic Peninsula in 2002, glaciers sped up by a factor two to six due to the loss of buttressing, leading to accelerated mass losses. This was followed by a rapid thinning of these glaciers, with a surface lowering of up to 38 m recorded a year after the ice shelf collapse over a period of only 6 months (Scambos et al. 2004). The thinning of the glaciers has persisted for many years after the ice shelf collapse and propagated further upstream with the 10 m year⁻¹ thinning contour propagating at a speed of 2 km year⁻¹ between 2006 and 2011 (Berthier et al. 2012).

Partitioning ice dynamics losses between their submarine melting and calving components reveal that submarine melting of tidewater glaciers' floating ice tongues and ice shelves accounts for about half of Antarctica's dynamic ice losses (Depoorter et al. 2013) and a quarter of Greenland's dynamic ice losses (Benn et al. 2017) with calving losses accounting for the remainder dynamic losses. Overall, ice losses in Antarctica are mainly caused by ice dynamics processes while in Greenland, ice losses are equally split between SMB and ice dynamics. However, in recent years, Greenland's mass loss has been dominated by reduced SMB as surface melt has intensified since the 2000s (Hanna et al. 2020) from a change in atmospheric circulation pattern favouring more frequent blocking events (Delhasse et al. 2018), leading to increased meltwater runoff. Both ice dynamics and SMB processes will remain important drivers of future Greenland's mass loss with SMB predicted to decrease—and could even become negative around 2055 in a high-end warming scenario, with snowfall accumulation during winter no longer compensating for meltwater runoff in summer (Noël et al. 2021)—and marine terminating glaciers predicted to retreat further inland, especially in northwest and central west Greenland (Choi et al. 2021). In Antarctica, ice dynamics will continue to dominate ice losses; however, it remains uncertain to which extent SMB will modulate these dynamics ice losses (Seroussi et al. 2020). Finally, as the balance between SMB and ice dynamics processes remains uncertain in the future, it is important to compare model projections to observations using the four decades of mass balance record available from satellite observations. Such comparison demonstrated the importance of including short-term variability in atmospheric and ocean warming in model simulations in order to reproduce the observed rates of Greenland and Antarctica mass change (Slater et al. 2020).

2.3 Basal Mass Balance

Basal mass balance refers to ice losses occurring at the base of the ice sheets that can arise primarily from geothermal heat flow, from frictional heat through basal shear stress and basal motion, and from viscous heat dissipation from the injection of surface meltwater to the bed (Young et al. 2022). The geothermal heat flow (GHF) refers to the transfers of heat from the Earth's mantle and crust to the surface (Burton-Johnson et al. 2020) and has been estimated by combining the very few temperature profiles available from deep ice-core drilling sites with a thermal model (e.g. Pattyn 2010), with a global seismic model (Shapiro and Ritzwoller 2004), or by using a magnetic field model based on satellite magnetic data (Fox-Maule et al. 2005). These models are in good agreement at the ice sheet scale, but at the local scale, differences between the two latter models range between 30 and 140% (Larour et al. 2012). Next, frictional heat is generated when the ice slides over its bed and can be estimated through inverse modelling using an ice flow model to invert

for observed surface velocities (e.g. Gillet-Chaulet et al. 2012; Morlighem et al. 2013). Finally, viscous heat dissipation is generated when surface meltwater reaches the bed. The amount of surface meltwater susceptible to infiltrate the subglacial system is usually estimated from a regional climate model, and the flow of water at the bed can be modelled using a simple routing model with water following the hydraulic potential gradient, itself dependent on the bed topography and thickness of the overlying ice (Mankoff and Tulaczyk 2017) or by a model that solves explicitly for the flow of water within subglacial conduits (e.g. Werder et al. 2013; de Fleurian et al. 2016). Basal melting generates meltwater underneath the ice sheets which constitutes a source of mass loss that has been estimated to 21.4 ± 4.4 Gt year⁻¹ in Greenland corresponding to 8% of Greenland's total mass loss (Karlsson et al. 2021) and to 65 Gt year⁻¹ in Antarctica, corresponding to 3% of Antarctica surface accumulation (Pattyn et al., 2010). Basal mass balance is thus much smaller than the other components of the ice sheets mass balance. However, Karlsson et al. (2021) found that basal melt increased by 2.9 ± 5.2 Gt during the first decade of the 2000s, suggesting that the contribution of basal melting might increase in a warmer climate. In addition, the presence of meltwater at the bed lubricates the base of the ice sheets, but can also modulate the amplitude of seasonal ice flow (Sundal et al. 2011) and has thus important implications for ice dynamics. Finally, subglacial meltwater can enhance melting at the grounding line as subglacial water released to the ocean can form a buoyant plume, entraining warm and salty ocean water close to the ice front (Jenkins et al. 2011; Le Brocq et al. 2013). While there have been some recent advances in quantifying the basal mass balance of the ice sheets, the thermal state of the base of the ice sheets (MacGregor et al. 2016) and subglacial conditions remain uncertain as there exist very few direct observations of these processes.

3 Measuring Ice Sheet Mass Balance from Space

Satellite observations have greatly advanced our understanding of the processes responsible for changes occurring across Antarctica and Greenland, particularly since the launch of a new generation of satellites in the 1990s, starting with the launch of ERS-1 (European Remote Sensing) in 1991 capable of mapping the ice sheets up to 82° latitudes. Earth Observations have been instrumental in detecting changes in ice sheet flow, thickness, mass, or grounding line location. In combination with numerical modelling, the physical processes responsible for the changes detected using satellite data can be better understood, which in turn can improve simulations of Antarctica's and Greenland's past, present, and future evolutions. Ice sheet mass balance at the continental scale can now be routinely estimated through three methods based on satellite observations: from observations of ice flow velocity combined with estimates of SMB in the mass budget method, or from repeated altimetry observations of surface elevation changes, or from observations of gravitational attraction fluctuations.

3.1 Mass Budget Method

The mass budget method, also called the 'input–output' method, consists of estimating the SMB and ice discharge components separately before differencing these two terms to derive the total mass balance following Eq. 1. As seen previously, the SMB term is estimated from regional climate models. On the other hand, ice discharge—the flux of solid

ice that is transported from the ice sheets to the ocean—is measured using satellite observations of ice velocity and measurements of ice thickness at the grounding line. Ice discharge thus has to be estimated for every glacier drainage basin that falls within the area over which to estimate mass balance. This entails positioning ‘ice flux gates’—virtual lines across which the ice is flowing into the ocean.

Identifying grounding line locations is thus critical when measuring ice discharge as their locations are used to position the flux gates. Importantly grounding lines determine the lateral extent of the ice sheets and are indicators of the stability of the ice sheets. Satellite measurements of the displacement of the floating ice shelves and ice tongues caused by ocean tides have been successfully used to identify the junction between grounded and floating ice: as the floating ice shelves or ice tongues move with ocean tides, they experience a vertical cyclic motion synchronous with the rise and fall of ocean tides, unlike the grounded ice which is not sensitive to tidal motion (Rignot 1996). Surface displacement can be either measured using differential satellite synthetic aperture radar interferometry (DInSAR)—in which two radar interferograms of the same area but acquired at different times are differenced together to extract surface displacement (Rignot et al. 2011a). Alternatively, the grounding line location can be measured using high resolution surface elevation change data from satellite laser altimetry (Fricker et al. 2009), or from the break in slope between the flat ice shelf and the grounded ice sheet identified from satellite radar altimetry (Hogg et al. 2018).

Ice velocity is measured inland from the grounding line location using satellite optical or radar imagery (Fig. 2). The first satellite measurements of ice velocity were made using images acquired by the optical satellite Landsat (Bindshadler and Scambos 1991); however, optical imagery can be used only at daylight and in absence of clouds, which means that it cannot be used for half of the year when the Polar Regions are plunged in darkness. On the

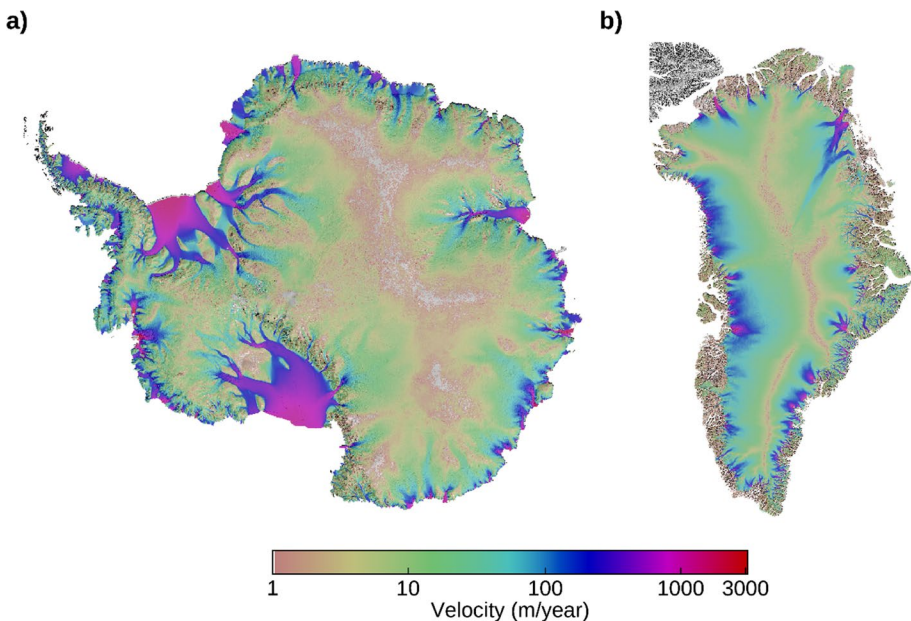


Fig. 2 Maps of **a** Antarctic and **b** Greenland Ice Sheet ice velocity derived from satellite radar interferometry (InSAR) data. Data from Rignot et al. (2011b) and Joughin et al. (2010)

other hand, radar sensors, which operate at microwave frequencies and can thus penetrate through clouds and provide an all-time monitoring of the Polar Regions, have been extensively used since the launch of ERS-1 in 1991. Since then, more satellite missions have been launched with the launch of ERS-2 (1995), Radarsat-1 (1995), Envisat (2002), ALOS (2006), Radarsat-2 (2007), TerraSAR-X (2007), TanDEM-X (2010), ALOS -2 (2014), Sentinel-1A (2014), and Sentinel-1B (2016) all carrying a synthetic aperture radar (SAR) instrument. In parallel, more optical satellites have also been launched, notably Landsat-7 (1999) and Landsat-8 (2013). Ice velocity is measured from sequential images acquired over the same area at different times using feature and speckle tracking techniques (Joughin 2002) or using the interferometric phase of SAR measurements (Mouginot et al. 2019b). Feature-tracking techniques consist of tracking persistent surface features, such as cracks or crevasses on the surface of glaciers and ice shelves, in a series of optical or radar images in order to deduce at what speed they are displaced. In the absence of visible features, speckle-tracking techniques have been developed for SAR images and are based on tracking the ‘salt and pepper’ or speckle patterns in sequential images using image cross-correlation. These two tracking techniques are well suited for measuring ice velocity especially in areas of fast ice flow as they have errors of the order of a few meters per year which is acceptable in those areas where ice velocity is typically hundreds of meters per year. On the other hand, in the interior of the ice sheets, where ice velocity is much smaller (typically about tens of centimetres per year), the level of precision of tracking techniques is not sufficient. In this case, to achieve a higher precision, the interferometric phase acquired by multiple SAR sensors at different look angles can be used instead as the precision of the resulting ice velocity fields is 10 times higher than when derived using tracking techniques. Applying this technique to the whole interior of the Antarctic Ice Sheet is now possible thanks to the multiple SAR sensors operating over the continent, acquiring scenes from ascending and descending tracks and from left and right looking angle tracks (Mouginot et al. 2019a, b). However, this is restricted to slow-moving areas as the interferometric phase unwrapping cannot be performed where the terrain is rapidly deforming and the signal coherence is thus lost.

Finally, the ice thickness at the grounding line needs to be known to calculate the volume of ice that is being discharged to the ocean. Usually measurements of ice thickness close to the grounding line are sparse and come from airborne surveys from gravimeters or from ground penetrating radars deployed during field campaigns. In addition, high-resolution surface elevation measurements from satellite altimetry or from DEMs can be used to correct for thickness changes over time. Ice discharge datasets for Greenland are available from King et al. (2020), Mouginot et al., (2019a, b), and Mankoff et al. (2020) and for Antarctica from Rignot et al. (2019).

Beyond estimating mass balance, the mass budget method provides a direct partitioning of ice sheet mass changes into SMB and ice dynamics processes, which enables to track the origin of the mass loss (or gain) over time. However, comparing two large terms implies that even a small relative error in either SMB or discharge can lead to a large relative error in mass balance. In particular, estimating ice discharge requires measurements of grounding line location, ice velocity, and ice thickness, which are not always available at every glacier or which cannot be updated regularly. In particular, ice thickness measurements are quite sparse in both space and time. As there are hundreds of glaciers in Antarctica and Greenland, ice discharge is usually determined over as many glaciers as possible where good estimates of ice velocity and ice thickness are available and extrapolation techniques are used over unobserved glaciers to provide a mass balance estimate at the continental scale. More recently, Mankoff et al. (2021) have accounted for the basal mass balance in their mass budget estimate for Greenland, which

is usually neglected as the magnitude of BMB is much smaller than the SMB and discharge terms, but still accounts for an additional mass loss of 24 Gt year^{-1} in Greenland.

3.2 Altimetry

Repeated radar or laser altimetry measurements from airborne and spaceborne platforms allow us to track changes in ice thickness over time and are therefore a powerful tool for studying ice sheet processes. Satellite altimetry has revealed spatial patterns of surface elevation change at fine (kilometre scale) spatial resolution across the vast majority of the Greenland and Antarctic ice sheets, showing that thinning is concentrated at the margins of the ice sheets (Fig. 3) (e.g. McMillan et al. 2016; Pritchard et al. 2009). Combined with a knowledge of the density of snow, firn, and ice, volume change estimates derived from satellite altimetry can be converted to mass changes.

Satellite altimeters transmit electromagnetic pulses towards the Earth's surface and record the two-way travel time of the signal (from the satellite to Earth and back to the satellite) as well as its magnitude over time. From this return echo or 'waveform', the distance from the satellite to the observed surface (the range) can be precisely measured. The success achieved in satellite oceanography altimetry encouraged the application of radar altimetry to land ice surfaces, which is complicated by the complex topography of the ice sheets. ERS-1 was the first mission with the explicit aim of monitoring the polar ice sheets, surveying Greenland and Antarctica up to 81.5° latitudes, which allowed the creation of the first complete map of surface elevation change of Antarctica (Wingham et al. 1998). Following this, several radar altimeters recording data over the ice sheets were launched

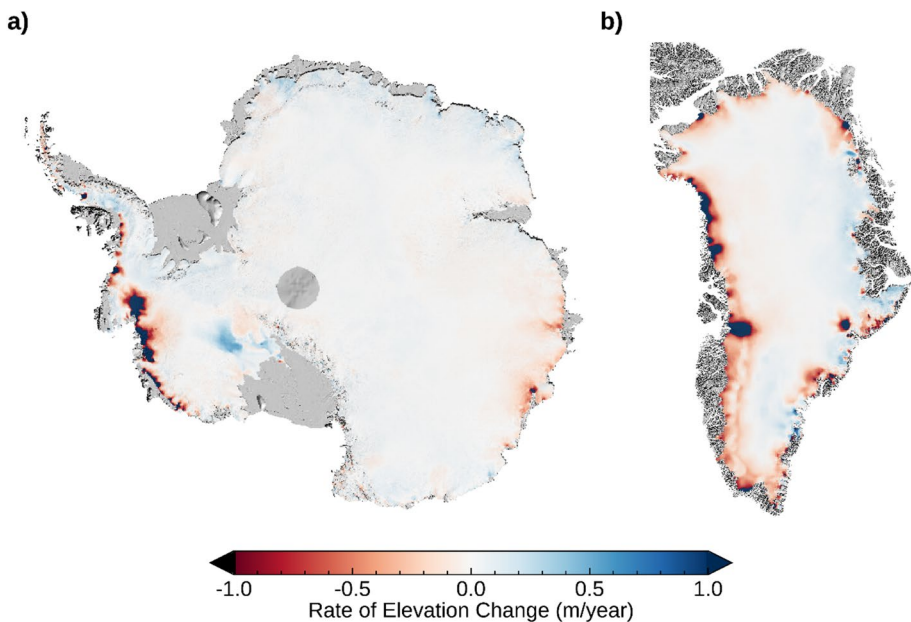


Fig. 3 Maps of **a** Antarctic and **b** Greenland Ice Sheets rates of surface elevation change between 2010 and 2021 derived from CryoSat-2 satellite radar altimetry. Antarctica elevation change data are from Shepherd et al. (2019) and Greenland data from Otosaka et al. (2021)

including ERS-2 (1995), Envisat (2002), CryoSat-2 (2010), AltiKa (2013), and Sentinel-3 (2016). CryoSat-2 in particular can map the ice sheets up to 88° latitudes and benefits from an interferometric mode, which allows more accurate measurements over the margins of the ice sheets. In addition to radar altimeters, laser altimeters have also been launched in space with the first spaceborne laser altimeter, ICESat, launched in 2003. The lidar system embarked on ICESat consists of three lasers, which had been operated one at a time during 18 episodic campaigns ranging from 18 to 55 days in duration covering latitudes up to 86° N/S and stopped operating in October 2009 after the failure of its last laser (Abshire et al. 2005). More recently, its follow-on, ICESat-2 was launched in 2018, embarking a photon-counting laser altimeter operating in the green light, surveying latitudes up to 88° (Markus et al. 2017). ICESat-2 overcomes the issues encountered by its predecessor and has been successfully used to measure surface elevation changes at fine spatial (Smith et al. 2020) and temporal scales (Adusumilli et al. 2021). While both radar and laser altimeters measure the range, radars are sensitive to the contrast in dielectric properties of the medium illuminated while lasers are sensitive to the upper optical surface at the top of the snow surface and do not penetrate into the snowpack. However, laser data are more sensitive to atmospheric conditions and cannot penetrate through the cloud cover, limiting the data acquisition in the presence of thick clouds or blowing snow (Palm et al. 2011). On the other hand, radar altimeters provide measurements in all weather conditions. Other differences between radar and laser altimetry relate to different footprints of the instruments. Satellite laser altimeters have a much smaller footprint (of the order of tens of meters), which results in a finer precision of the range measurement (to the decimal level) than that of radar altimeters. Over the ice sheets, the terrain topography is far from homogeneous within the satellite radar altimeter's footprint especially over the margins of the ice sheets where fluctuations in surface elevation can reach up to tens of meters over a few kilometres. This requires to correct altimetry measurements for this slope-induced error as if uncorrected, it can lead to errors of the order of tens of meters. Several geometric corrections have been developed which usually make use of an external digital elevation model to relocate the signal to its true location of origin (Otosaka et al. 2019; Roemer et al. 2007). A further complication over the ice sheets is the penetration of the radar wave into the snowpack. The radar signal can penetrate into the snowpack up to 12 m below the ice sheet surface, depending on the physical properties of the snowpack and the frequency of the sensor (Rémy et al. 2015). As a consequence, the radar waveform is the sum of a surface and volume echo (Ridley and Partington 1988). The surface echo is modulated by the snow density and surface roughness while the volume echo is the result of ice grain size and internal layering in the snowpack (Rémy et al. 2014). A sudden change in the snowpack properties can thus bias the surface elevation retrieved from satellite radar altimeters. This issue was illustrated during the Greenland melt event of 2012, following which a thickening of 0.5 m of the interior of the ice sheet over a period of only 5 months was observed from CryoSat-2 (Nilsson et al. 2015). However, this step in elevation change was caused by the formation of a refrozen ice layer at the surface of the ice sheet following the melt event rather than being an actual elevation change caused by snowfall accumulation. To mitigate this effect, different algorithms have been designed to better locate the surface from the radar waveforms (Otosaka et al. 2020). Alternatively, this effect can be compensated for by separating the surface and volume scattering components of radar echoes to directly estimate the radar penetration depth (Slater et al. 2019).

By repeatedly measuring surface elevation from satellite altimetry, it is possible to estimate temporal changes in surface elevation across the ice sheets. The very first method employed to derive surface elevation change of the ice sheet is based on the analysis of

differences in elevation at crossover points, where ascending and descending orbits cross each other (e.g. Wingham et al. 1998; Zwally et al. 1989). However, restricting the calculation of surface elevation changes to crossover points does not provide a complete coverage of the ice sheets and therefore limits the subsequent derivation of volume change or mass balance from crossover points. Instead, the repeat-track (Flament and Rémy 2012) and plane-fit methods (McMillan et al. 2016), which consist of grouping data points on their spatial proximity either along segments of satellite tracks, within regular grid cells, or within triangular facets were developed (Felixson et al. 2017). To derive time-series of surface elevation change, a least-square model is fitted to the elevation measurements that fall within each group of data. These multi-parameters models are dependent on the topography of the terrain, time of the measurement, heading of the satellite, and waveform parameters (Flament and Rémy 2012; Simonsen and Sorensen 2017).

Altimeters measure the integrated change in surface elevation, which arises from a combination of SMB, ice dynamics processes, and hydrological processes but also includes changes in the firn layer thickness and rebound from the solid Earth's response to past and present ice sheet mass changes, which are not associated with a mass change. The former results in elevation changes of the order of a few millimetres per year. The vertical displacement induced by the GIA can be corrected using uplift rates estimated by a GIA model (e.g. Caron et al. 2018; Peltier 2004), and the displacement induced by present-day mass changes can be modelled using Green's functions (Farrell and Clark 1976). Next, accumulated snow at the surface of the ice sheet compacts into firn—the intermediate stage between snow and glacial ice—thus increasing its density. Snow deposited at the surface of the ice sheet has a density of about 315 kg m^{-3} (Fausto et al. 2018) and contains a large amount of air. As more snow is deposited at the surface, air between firn pore spaces is gradually squeezed out under the action of gravity, progressively increasing the density of the firn. High values of firn air content are found in areas of high accumulation where the firn layer is buried quickly, resulting in a thick firn layer with remaining air bubbles while low values of firn air content are found in regions where surface melting is important (Ligtenberg et al. 2014). Densification of the firn results in a decrease in surface elevation with no associated mass change and thus needs to be accounted for before converting the elevation changes measured by altimeters to mass changes. To do so, firn densification models (FDM) are used to estimate the volume change associated with firn densification processes separately. FDMs are forced at the surface using a regional atmospheric climate model and simulate the transfer of mass and energy within the firn column through processes of compaction, meltwater percolation, and refreezing and provide estimates of firn air content (FAC) and density as a function of time and depth (e.g. Kuipers Munneke et al. 2015). FDMs are calibrated against in-situ firn cores or airborne radar records of annual layering (Simonsen et al. 2013). However, their performance has been assessed by comparing firn height changes to satellite altimetry height changes in areas where SMB and firn processes are the main drivers of surface elevation changes and these comparisons have shown that there remain significant differences between modelled and observed elevation changes (Verjans et al. 2021; Smith et al. 2022). By removing the volume associated with FAC change from the total volume change measured by altimeters, the resulting ice volume change can then be directly converted to a mass change using the density of ice. Alternatively, the conversion of altimetric volume changes to mass changes can be performed based on the assumption that volume changes in ice dynamical areas occur at the density of ice and elsewhere at the density of snow (Shepherd et al. 2019).

3.3 Gravimetry

Satellite orbits are primarily controlled by Earth's gravitational attraction. This allows to infer Earth's gravity field from observations of orbit geometry. While this principle has been realised since the early space age, the Gravity Recovery and Climate Experiment (GRACE) mission (Tapley et al. 2019) allowed, for the first time, to determine the global gravity field accurately enough to reveal its tiny temporal changes at a resolution of a few hundred kilometres.

GRACE operated from 2002 to 2017 and the similar GRACE-Follow-On (GRACE-FO) mission (Landerer et al. 2020) was launched in 2018. Each mission consists of twin satellites that follow each other in a low-altitude, near-polar orbit at a 200 km distance. Variations in this distance are measured at sub-micrometre precision by a microwave ranging system (complemented by a laser ranging system at GRACE-FO). Additional instruments allow the determination of the orbit, the attitude, and non-gravitational accelerations. Measurements from GRACE or GRACE-FO (both referred to as GRACE in the following) collected over a certain time interval—typically a month—are processed by processing centres to determine the global gravity field for this given month. Users can then analyse the temporal gravity field variations reflected by a sequence of monthly solutions to infer mass variations.

In general, Earth's gravity field (and its changes in time) cannot be uniquely attributed to a mass distribution in the Earth system (and its temporal changes, respectively). Uniqueness can be enforced by assuming the mass redistribution to occur in a thin layer at the Earth surface (Wahr et al. 1998), which is justified for changes of land ice, land water, and ocean masses. Hence, by neglecting their radial dimension, mass changes are expressed in terms of surface mass density (mass per surface area, in units of kg m^{-2}) or the equivalent height of a water layer (mm water equivalent). Importantly, in order to infer on surface mass changes and their attribution to ice mass balance, it is necessary to account for mass redistributions in the Earth's interior due to the glacial isostatic adjustment (GIA). Therefore, GIA is usually corrected for by using results of geophysical forward modelling (Shepherd et al. 2018, 2020; Whitehouse 2018). Atmospheric mass variation effects as well as effects of ocean dynamics are accounted for already in the gravity field determination step (Dobslaw et al. 2017). The spatial resolution at which mass changes can be inferred from GRACE without additional information is limited to a few hundred kilometres and larger. Indeed, the gravitational pull on the satellites is an integrated effect of masses and has vanishing sensitivity to their small-scale spatial distribution. As GRACE measurements are not related to discrete locations or pixels, no single number can be put on the GRACE resolution capability. GRACE gravity field errors depend on the spatial scale, or 'wavelength', and increase rapidly with decreasing wavelength. The errors also exhibit non-isotropic characteristics (meridional striping) and latitude dependence, both related to the orbital sampling geometry (Wouters et al. 2014).

GRACE gravity field solutions are commonly represented in the spectral domain, according to their non-discrete and wavelength-dependent nature. Specifically, a spherical harmonic (SH) representation is used to decompose the gravity field into a set of basis functions, each being a continuous global pattern associated with a certain spatial wavelength. The analysis centres of the GRACE/GRACE-FO Science Data System (SDS)—the University of Texas at Austin Center for Space Research (UTCSR), the Helmholtz Centre Potsdam German Research Centre for Geosciences (GFZ), and the Jet Propulsion

Laboratory (JPL)—provide monthly global gravity field solutions (Level-2) that consist of SH (Stokes) coefficients (C_{lm}, S_{lm}) up to degree l and order m , with typical values for l and m of 60 or 96 (Bettadpur 2018; Dahle et al. 2019; Yuan 2018). Similar series of monthly solutions are provided by other analysis centres, and the quality of some of these alternative products (such as by Graz University of Technology, Kvas et al. 2019) is competitive to the SDS products (Ditmar 2022). Moreover, the Combination Service for Time-variable Gravity Fields (COST-G; Jäggi et al. 2020) generates consolidated monthly gravity field solutions by combining solutions of different analysis centres using variance component estimation.

Users analyse such series of GRACE monthly solutions in order to determine mass changes within a discrete region of interest (such as an ice sheet or one of its drainage basins). Different methods have been developed for this analysis. Overall, the task is to find a compromise between retaining spatial resolution (hence retaining small-wavelength components) and reducing noise (which is large at small wavelengths). The noise in the GRACE gravity field solutions has a non-isotropic correlation structure, which manifests itself as north–south striping (Wouters et al. 2014). Reduction in this noise is commonly done by filtering and smoothing approaches ranging from isotropic Gaussian filtering (Wahr et al. 1998), empirical non-isotropic de-striping filters (Swenson and Wahr 2006) to filters that mimic a regularisation in the gravity field estimation process (Kusche et al. 2009). Such filtering, in turn, decreases the spatial resolution. The limitations in spatial resolution lead to so-called leakage errors (Swenson and Wahr 2002; Horwath et al. 2009; Velicogna and Wahr 2013). As a visual impression of leakage from maps of filtered surface mass densities, mass changes originally located inside the region ‘leak out’ into adjacent regions while, conversely, mass changes from outside the region ‘leak in’ into the region.

Methods to determine mass changes from GRACE SH solutions have been often distinguished as belonging to the direct approach or to the inverse approach (e.g. Döhne et al. 2023). By the direct approach (or regional integration approach), surface mass density changes inferred from gravity field changes are integrated over the region of interest. The procedure usually involves filtering and other amendments of the satellite gravimetry input fields and of the weight function used in the integration. The inverse approach (or forward-modelling approach, or mascon—mass concentration—approach) prescribes a set of predefined mass change patterns and determines their amplitudes to fit the observed gravity field changes. Döhne et al. (2023) elaborate on a framework to characterise and compare methods from both approaches, and they recall that leakage effects arise with both approaches.

An alternative to using SH gravity field solutions consists in mascon solutions provided by some analysis centres, such as CSR (Save et al. 2016), JPL (Watkins et al. 2015), and the Goddard Space Flight Center (GSFC) (Luthcke et al. 2013; Loomis et al. 2019a). These mascon solutions directly determine mass redistributions from the GRACE inter-satellite ranging data without using a gravity field solution as an intermediate product. The mascon solutions are represented as mass changes of discretely delineated patches. These mascon solutions result from specific processing choices made for resolving the integrative information present in the GRACE measurements. Hence, users do not need to make such choices, but at the same time, they have no control on these choices.

An overview over some recent GRACE-based ice sheet mass change estimates and references to different methodologies applied are given by Otsuka et al. (2023). Time-series of GRACE ice sheet mass change estimates (Fig. 4c) do not only show significant long-term trends, but, owing to their monthly resolution, they also resolve seasonal variations (prominent in Greenland) and distinct inter-annual features (such as effects of extreme Greenland summer melting in 2012, or of excess snow accumulation in East Antarctica in

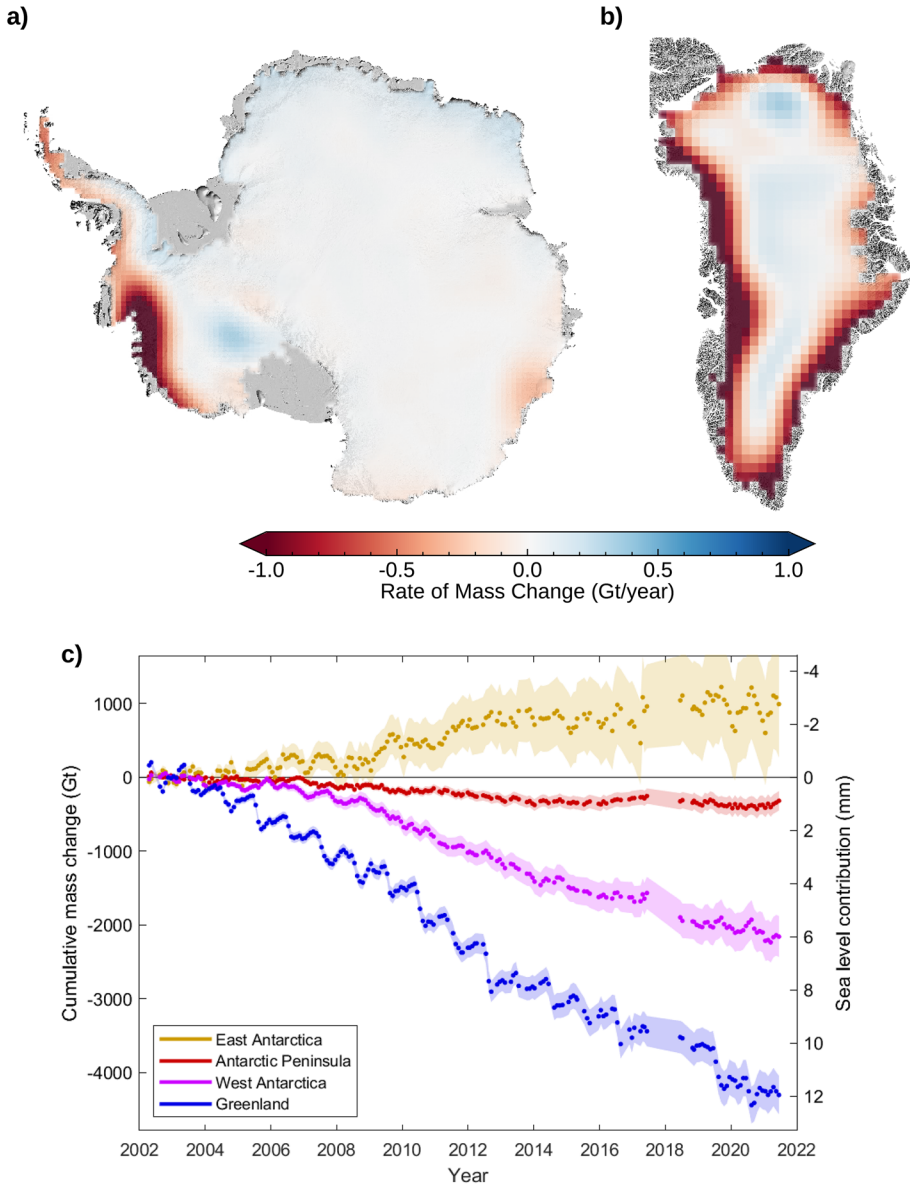


Fig. 4 Maps of **a** Antarctic and **b** Greenland Ice Sheets rates of mass change between 2010 and 2021 (the same period as used in Fig. 3) derived from GRACE and GRACE-FO satellite gravimetry. **c** Cumulative mass change time series of the East Antarctic Ice Sheet, the West Antarctic Ice Sheet, the Antarctic Peninsula, and the Greenland Ice Sheet. One-sigma uncertainties (shaded) grow over time due to systematic uncertainties of the long-term trends, while the noise level and quality of the monthly values remain similar over the entire period. Data from Groh and Horwath 2021 and Döhne et al. 2023

2009 and 2011), which agree with results of SMB modelling (Velicogna et al. 2020; Willen et al. 2021) and satellite altimetry (Horwath et al. 2012; Schröder et al. 2019). On the other hand, the gridded representation of mass changes illustrates the effective resolution on the

order of 300 km (Figs. 4a and b). The grids provide a smoothed (or filtered) representation of the true mass-change patterns.

Uncertainties in GRACE ice mass change estimates arise from different sources (Horwath and Dietrich 2009; Velicogna and Wahr 2013). First, errors on the monthly gravity field solutions propagate into the final mass change estimates, with larger gravity field uncertainties for small-wavelength components. In addition, a limited sensitivity of GRACE applies to largest spatial scales. Namely, GRACE is insensitive to shifts of the centre of gravity of the Earth, dominated by the water masses redistributed at the Earth surface. GRACE also has reduced sensitivity to the dynamic flattening component. These largest scale components (referred to as SH degrees 1 and 2) are usually determined by combinations of GRACE results, model assumptions, and satellite laser ranging (Loomis et al. 2019b; Sun et al. 2016). As a second error category, leakage errors arise from the limited spatial capability of satellite gravity measurements. Mass changes occurring outside a target basin (or a pixel) affect the mass change estimate for that target basin (or pixel, respectively). Likewise, mass changes inside the target basin (or pixel) may be underrepresented or overrepresented in the estimate. Without any a priori constraints on the mass change patterns, such leakage errors cannot be completely avoided. As a third uncertainty category, corrections for signals superimposed to ice mass changes come with their errors, with the GIA uncertainty being particularly important (Shepherd et al. 2018, 2020).

Altogether, the uncertainty of the mean trend for the Antarctic Ice Sheet as a whole has been assessed on the order of ± 40 Gt year⁻¹ (Barletta et al. 2013; Groh and Horwath 2021; Shepherd et al. 2018), about 40% of the actual signal. This uncertainty is dominated by the GIA uncertainty, manifested by a large spread between alternative GIA models. Uncertainties in the SH degrees 1 and 2 components are also important. For single Antarctic drainage basins, such as Pine Island Glacier basin, leakage may become the dominant error source (Groh and Horwath 2021), which reflects the limited separability of adjacent basins. For the Greenland Ice Sheet as a whole, uncertainties associated with GIA, low-degree components, and leakage (such as associated with peripheral glaciers) are all important yet smaller than for the Antarctic Ice Sheet (Barletta et al. 2013; Shepherd et al. 2020). They add up to an assessed uncertainty of multi-year trends on the order of ± 20 Gt year⁻¹. For individual Greenland drainage basins, again, leakage becomes a dominant error source (Groh et al. 2019).

In summary, satellite gravimetry realised by GRACE and GRACE-FO at monthly resolution is unique for its direct sensitivity to mass changes and for the integrative nature of the information it provides. These characteristics are pros and cons at the same time. The separation of different signals, either superimposed vertically or proximate geographically, requires additional assumptions, modelling results, or observations. Combining GRACE with such complementary information is a promising way to downscale the GRACE information (Forsberg et al. 2017; Sasgen et al. 2019; Kappelsberger et al. 2021) or to separate ice mass changes from GIA (Engels et al. 2018; Willen et al. 2020, 2022; Scheinert et al. 2023). Future gravity mission projects (Haagmans et al. 2020) bear the perspective on continuity of satellite gravimetry at even better accuracy and spatial resolution as an essential component in ice sheet mass balance assessments.

3.4 Strengths and Limitations of Different Mass Balance Estimation Techniques

The three techniques described above have all contributed to advancing our understanding of the physical processes leading to ice sheet mass loss and gain and have established our

capability to monitor ice sheet mass balance from space. However, each technique has its own strengths and limitations.

The mass budget method provides the longest record of ice sheet mass changes thanks to the archive of optical images acquired by Landsat in the 1970s and 1980s. Another advantage of the mass budget method is that it provides estimates of ice discharge and SMB separately within individual glacier drainage basins, which can be used to investigate the influence of ocean- and atmosphere-driven processes on rates of mass change. In addition, a recent improvement in the mass budget method is the inclusion of the basal mass balance component (Mankoff et al. 2021). However, there are unique challenges associated with estimating those three components. First, observations of surface velocities, although available before the 1990s, are limited in their coverage of the ice sheets, and therefore, extrapolation of ice discharge measured from a few glacier basins to provide an ice sheet scale mass balance estimate is required. An important limitation in computing ice discharge is the limited availability of ice thickness measurements all around the coast of Greenland and Antarctica. Second, SMB estimates are extracted from a regional climate model, but model inter-comparisons have shown that while there is a good agreement in total SMB values, there are significant differences in individual SMB components. For instance, in Greenland, there is a standard deviation of $20.7 \text{ Gt year}^{-1}$ between the three commonly used RCMs (HIRHAM, MAR, and RACMO), but standard deviations of $30.6 \text{ Gt year}^{-1}$ and 108 Gt year^{-1} for the snowfall and runoff components, respectively (Fettweis et al. 2020). Similarly in Antarctica, a model inter-comparison found a standard deviation of $49.4 \text{ Gt year}^{-1}$ between the three RCMs, and standard deviations of $71.3 \text{ Gt year}^{-1}$ and $31.3 \text{ Gt year}^{-1}$ for the precipitation and sublimation components, respectively (Mottram et al. 2021). Finally, only one Greenland mass budget estimate so far has accounted for basal mass balance (Mankoff et al. 2021). This is a challenge as there are no direct observations of basal melt rates and both the thermal state of the bed and subglacial conditions are poorly constrained. Avenues for further research to improve estimates of melting underneath Antarctica and Greenland include investigating the temporal evolution of basal melt rates throughout the satellite record and in a warming future. While a recent refinement in mass budget estimates is the improvement in their temporal resolution, with most estimates of ice discharge now provided at monthly resolution (e.g. King et al. 2018; Mankoff et al. 2021), the spatial resolution of mass budget estimates remains at the glacier basin scale.

In comparison, altimetry estimates are provided at both fine spatial and temporal resolution, resolving the pattern of elevation changes across Greenland and Antarctica at a resolution of a few kilometres over monthly epochs, which has proved critical for both detecting local glaciological changes, but also for initiating ice sheet models. While altimetry provides a record of elevation and mass changes since the 1990s, CryoSat-2 and ICESat-2 in particular allow for more precise retrievals of surface height changes even in the ice sheet margins, where most of the mass loss occurs. Current limitations include the conversion of volume changes to mass changes as this requires knowledge of the density of the medium lost (or gained), which in theory can range from the density of snow (350 kg m^{-3}) to the density of ice (917 kg m^{-3}). To address this challenge, firn compaction models to correct for FAC (e.g. Smith et al. 2020) or to separate elevation changes into changes driven by accumulation and ice dynamics occurring at the densities of snow and ice, respectively (Shepherd et al. 2019), have been used. However, a comparison of FAC extracted from HIRHAM, MAR, and RACMO has shown that despite an overall agreement within 12% of FAC observations from firn cores, this agreement varies regionally and is model-dependent (Vandecrux et al. 2019). Finally, another limitation pertaining to radar altimetry measurements is the potential impact of temporal and spatial variations in radar penetration into

the snowpack on surface height measurements. Some post-processing strategies based on retracking and analyses of time-series of waveform parameters have been devised, but this could be further addressed through comparisons of CryoSat-2 radar altimetry and ICE-Sat-2 laser altimetry data.

Lastly, gravimetric mass balance estimates are available since the launch of GRACE in 2002. Compared to the other techniques, gravimetry has the advantage of directly measuring mass changes, but these measurements also include the redistribution of mass due to the GIA, which needs to be removed with the aid of a model. A comparison of GIA models found a spread of GIA corrections of 20 Gt year⁻¹ in Greenland (Shepherd et al. 2020) and a range of corrections between 12 Gt year⁻¹ and 81 Gt year⁻¹ depending on the model used in Antarctica (Shepherd et al. 2018). The choice of model used thus has a large impact on the final mass balance estimate. Similar to the other techniques, gravimetry also measures ice sheet mass changes at high temporal resolution (monthly), but its spatial resolution is coarser (~300 km), which renders difficult the separation of mass change signals emerging from the ice sheets and their peripheral glaciers and ice caps, or between neighbouring glacier basins.

Comparing and aggregating ice sheet mass balance estimates from these different techniques lead to greater certainty (Shepherd et al. 2012). Comparisons of ice sheet mass balance estimates have found a good level of agreement between the three independent techniques, with a standard deviation of 19 Gt year⁻¹ and 79 Gt year⁻¹ between estimates of Greenland and Antarctica mass balance, respectively, during their overlap period (Otosaka et al. 2023). The larger spread of estimates in Antarctica originates from East Antarctica where the mass balance signal is small compared to fluctuations in SMB in this region, but the agreement between techniques is high in both West Antarctica and the Antarctic Peninsula, with standard deviations of 18 Gt year⁻¹ and 16 Gt year⁻¹, respectively. More recently, new approaches to combine these techniques together and take advantage of their respective strengths have been developed. These approaches include using a machine learning approach to calibrate radar and laser altimetry records to convert radar volume changes to mass changes (Simonsen et al. 2021), using satellite altimetry to improve the spatial resolution of the gravimetry record (Forsberg et al. 2017; Sasgen et al. 2019; Kappelsberger et al. 2021), or using the ice discharge component from the mass budget method to validate the partitioning of altimetry and gravimetry mass trends into their SMB and ice dynamics components (e.g. Diener et al. 2021).

4 Ice Sheet Mass Changes During the Satellite Era

As we have seen in the previous section, satellite techniques have been developed and used to study how glaciers around Antarctica and Greenland are evolving over time. Pine Island Glacier in West Antarctica is the largest contributor to Antarctica's ice losses, losing 58 Gt year⁻¹ in 2017 (Rignot et al. 2019) and has shown strong decadal variations in its flow, thickness, and grounding line location. Satellite radar interferometry observations have revealed that between 1992 and 2011, Pine Island grounding line retreated by 31 km (Rignot et al. 2014). Pine Island Glacier sped up until 2009, with ice velocity reaching peaks of 4000 m year⁻¹ (Joughin et al. 2016) and thinning rates exceeding 5 m year⁻¹ in the central trunk of the glacier close to the grounding line in 2009 (Konrad et al. 2017), after which the grounding line has stabilised (Mouginot et al. 2014). Since then, thinning in the fast-flowing trunk of the glacier has reduced by a factor three and the highest rates

of thinning are now instead found in areas of slow flow beyond the shear margins (Bamber and Dawson 2020). Variations in the flow of Pine Island Glacier are thought to be driven by thinning of its ice shelf due to ocean melting (e.g. Christianson et al. 2016; Dutrioux et al. 2014) and calving processes (De Rydt et al. 2021), leading to a reduction in ice shelf buttressing. Furthermore, satellite imagery has revealed the existence of crevasses and open fractures in the ice shelf shear zones during the past decade—first initiated in 1999 and rapidly expanding since 2016. The damage development over Pine Island has progressively weakened the ice shelf, enhancing ice shelf disintegration and promoting further grounding line retreat (Lhermitte et al. 2020). In Greenland, satellite imagery has shown that marine terminating glaciers from all sectors of the ice sheet have experienced pronounced retreat during the past decades, with this retreat likely starting in the 1990s and accelerating since then (Howat and Eddy 2011). Sermeq Kujalleq (formerly known as Jakobshavn Isbrae) is the largest contributor to sea-level rise from the Greenland Ice Sheet, accounting for 6.6% of the ice sheet total ice losses between 1972 and 2018 (Mouginot et al. 2019a). Sermeq Kujalleq has experienced sustained retreat and thinning for two decades before recently advancing and thickening again. Intrusion of warm water from the Irminger Sea in its fjord in 1997 likely triggered the breakup of its floating ice tongue (Holland et al. 2008) and subsequent speedup (Joughin et al. 2008) observed until 2016, when Sermeq Kujalleq started re-advancing and thickening due to cooling of the ocean temperatures in Disko Bay (Khazendar et al. 2019).

As shown so far, satellite observations are key to detect and interpret changes in Greenland and Antarctica's glaciers. In addition, it is now possible to track changes in ice sheet mass balance over time at the continental scale using either the mass budget method, satellite altimetry, or satellite gravimetry. Combining mass balance estimates derived from these three independent techniques has revealed that the Greenland and Antarctic Ice Sheets have collectively lost 7.6 ± 0.7 trillion tonnes of ice between 1992 and 2020 (Otosaka et al. 2023) (Fig. 5).

This satellite record shows that ice losses from the Antarctic Ice Sheet have accelerated during the past decades, rising from 70 ± 40 Gt year⁻¹ between 1992 and 1996 to 115 ± 55 Gt year⁻¹ between 2017 and 2020 (Otosaka et al. 2023). Unlike in Greenland—where ice

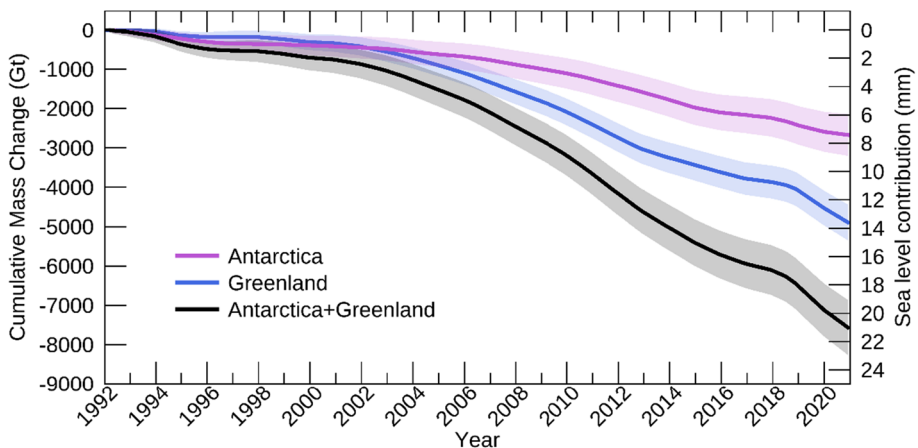


Fig. 5 Time-series of Antarctica and Greenland cumulative mass change derived from a combination of satellite gravimetry, satellite altimetry, and mass budget estimates. Data from Otosaka et al. (2023)

losses are equally split between ice dynamics and surface processes—most of Antarctica's ice losses are driven by submarine melting and iceberg calving, which lead to glacier speedup (Rignot et al. 2019). 86% of Antarctica's total ice losses originate from West Antarctica, with the rapid retreat and thinning of Pine Island and Thwaites glaciers due to ocean melting (Rignot et al. 2014; Shepherd et al. 2002), and almost a quarter of West Antarctica is now estimated to be in a state of dynamic imbalance (Shepherd et al. 2019). Ice losses at the Antarctic Peninsula increased by 25 Gt year^{-1} over the 1992–2017 period following the collapse of the Larsen B Ice Shelf (Rignot et al. 2004). On the other hand, East Antarctica has remained close to a state of balance at $3 \pm 15 \text{ Gt year}^{-1}$ between 1992 and 2020 (Otosaka et al. 2023).

Before the 1990s, the Greenland Ice Sheet was close to a state of balance with mass gain from snowfall accumulation balancing out mass losses from meltwater runoff and solid ice discharge into the oceans (Mouginot et al. 2019a). Since then, ice losses have accelerated due to increased ice flow of marine terminating glaciers and increased meltwater runoff, rising from $35 \pm 29 \text{ Gt year}^{-1}$ in the 1990s to 257 ± 42 between 2017 and 2020 (Otosaka et al. 2023) leading to widespread thinning at the ice sheet margins (McMillan et al. 2016). Ice losses from reduced SMB and increased solid ice discharge to the oceans contributed equally to total ice losses over the period 1992–2018. However, this partitioning of Greenland's mass loss has changed over time. In the early 2000s, ice discharge rose sharply primarily driven by the acceleration of outlet glaciers in northwest and southeast Greenland (Moon et al. 2012). However, after 2009 the main driver of Greenland's ice losses was the decrease in SMB, which accounted for 84% of the increase in mass loss, due to increased surface meltwater runoff (Enderlin et al. 2014).

5 Projections of Future Ice Sheet Mass Changes and Sea-Level Rise

As underlined so far, satellite observations over the Antarctic and Greenland Ice Sheets revealed their rapid and complex response to a warming climate. In addition, the considerable improvements in the availability and abundance of observations of ice sheet changes have resulted in an improved understanding of the key physical processes behind those changes and supported new refinements of ice sheet models (Goelzer et al. 2017; Pattyn et al. 2017). Community benchmark experiments, such as ISMIP-HOM (Pattyn et al. 2008) or the series of Marine Ice Sheet Model Inter-comparison Projects (MISMIPs) (Asay-Davis et al. 2016; Pattyn et al. 2012), have substantially advanced ice sheet modelling capabilities. Developments in recent years range from improved ice flow representation, to novel methods for discretisation of model domain or capabilities for ice margin and grounding line migration. These improvements are fundamental for capturing the motion of fast-flowing outlet glacier, ice streams and ice shelves. In parallel, efforts to improve the representation of interactions of the ice sheets with their surrounding climate have been made through the coupling of dynamical ice sheet models and climate models and the development of novel methods for representing ice sheet–atmosphere interactions and for ice sheet ocean parameterisations (Fyke et al. 2018; Nowicki and Seroussi 2018).

The recent Intergovernmental Panel on Climate Change (IPCC) Sixth Assessment Report (AR6) incorporates those recent progress and makes use for the first time of projections from model inter-comparison projects (MIP) such as the Ice Sheet MIP for the sixth Coupled Model Intercomparison Project (CMIP6) (ISMIP6, Nowicki et al. 2020, 2016) and the Linear Antarctic Response MIP (LARMIP2) (Levermann et al. 2020), instead of relying on single

model studies. In addition, it also uses emulators—statistical models based on Gaussian process regression linking model input and output parameters—to generate probability distributions of output parameters at untried inputs, in a way that is faster and less computationally intensive than running a very large number of complex model simulations. This allows us to sample a broader range of possible future climate and ice sheet modelling uncertainties than simulated with ice sheet MIPs (Edwards et al. 2021). However, the Greenland and Antarctic Ice Sheets still remain one of the most uncertain contributors to future sea levels (Fox-Kemper et al. 2021). For the Greenland Ice Sheet, the IPCC AR6 projected contribution to global mean sea-level rise until 2100 ranges from 0.01 to 0.1 m under a low emission scenario (SSP1-2.6) to 0.09–0.18 m under a high emission scenario (SSP5-8.5). On the other hand, the Antarctic Ice Sheet will likely contribute between 0.03 and 0.27 m under a low emissions scenario and 0.03–0.34 m under a high emission scenario by 2100 based on the IPCC AR6 projections. Beyond 2100, the two ice sheets will continue to lose mass, with greater contribution to global mean sea level projected under high emission scenarios than low emission scenarios.

The future evolution of the two ice sheets depends heavily on their local conditions and how a warming climate translates into changing atmospheric and oceanic conditions. In a warmer world, surface melt due to a warmer atmosphere will dominate ice loss from the Greenland Ice Sheet (Edwards et al. 2021; Goelzer et al. 2020; Payne et al. 2021). In contrast, warmer atmospheric conditions over Antarctica may result in increased snowfall resulting in a mass gain which could counter the mass loss triggered by warmer oceans (Seroussi et al. 2020; Payne et al. 2021; Edwards et al. 2021). Projections of polar climate, however, remain challenging, resulting in a spread of projected regional atmospheric and oceanic conditions (Barthel et al. 2020; Jourdain et al. 2020; Nowicki et al. 2020). Nonetheless, ice sheet model projections indicate that West Antarctica will continue to be vulnerable in a warmer world, in particular from the action of warmer oceans (Edwards et al. 2021; Levermann et al. 2020; Payne et al. 2021; Seroussi et al. 2020), such that dynamic losses driven by ocean warming and ice shelf disintegration will likely dominate Antarctica's future evolution.

Although ice sheets grow as a result of snowfall accumulation over thousands of years, ice sheets can lose mass rapidly once instabilities have been triggered. Ice sheets are also suspected to be vulnerable to positive feedback effects—marine ice sheet instability (MISI) and marine ice-cliff instability (MICI)—that would lead to a rapid acceleration in mass loss and irreversible retreat of the ice sheets in case of prolonged atmospheric and oceanic warming. However, the vulnerability of the ice sheets to these positive feedback effects remains unclear. MISI is associated with grounding line retreat on a retrograde bed slope, a mechanism that would reinforce itself as ice thickness increases inland thus increasing the ice flux as the grounding line retreats further (Ritz et al. 2015). Thwaites and Pine Island Glaciers basins in West Antarctica are suspected to already be undergoing this process (Joughin et al. 2014a). On the other hand, MICI is associated with a collapse of tall ice cliffs (~90 m) triggered by ice-shelf collapse, inducing a rapid and sustain retreat of the ice sheet (DeConto and Pollard 2016). While it would lead to a nonlinear response of the ice sheets and a more extreme sea-level rise contribution, it has not been observed previously and may not be needed to reproduce past variations in sea-level rise (Edwards et al. 2019). The IPCC AR6 recognised this potential for higher than projected sea-level rise on century timescale with a 'low confidence' or 'low probability' scenario characterised by deep uncertainty. This scenario includes, for example, the possibility that currently poorly understood processes leading to ice shelf disintegration or breakup could trigger these dynamical instability mechanisms in Antarctica or could result in faster than projected changes in the surface melt of Greenland (Fox-Kemper et al. 2021). Thus, sea-level contribution in the range of 0.09 to 0.59 m for Greenland and 0.02

to 0.56 m for Antarctica by 2100 cannot be excluded. By 2300, deep uncertainty in Antarctica's future could result in 13.54 m of sea level rise due to MICI.

6 Conclusions and Outlook

While the Antarctic and Greenland Ice Sheets were thought to be changing very slowly at the scale of millennia before the 1990s, advances in Earth Observations and ice sheet modelling have shown that the ice sheets are actually subject to rapid changes. This was highlighted with the sudden break-up and disintegration of Larsen B ice shelf in the Antarctic Peninsula in 2002 which occurred over the course of several months only. Recently, the Greenland Ice Sheet has also been experiencing rapid changes with several extreme surface melt events occurring in the past decade, with the most recent one in summer 2019, which led to a new record ice loss. The ice sheets are now losing mass six times faster than in the 1990s based on the three-decade long satellite record.

Satellite observations are key to ensure a continuous monitoring of these remote regions and new satellite missions as well as progress in the techniques used to extract and interpret information from satellite data have revolutionised the way we look at the ice sheets. Measuring ice sheet mass balance from space can now be done routinely using geodetic observations of ice velocity, changes in their volume, or gravitational attraction and independent estimates of ice sheet mass balance derived from the mass budget method, altimetry, and gravimetry have been shown to be in good agreement, which leads to a greater confidence in estimates of ice sheet mass balance and in their contribution to global mean sea level. This is critical as the ice sheets are predicted to become the largest contributor to global mean sea-level rise. However, large uncertainties remain regarding their projected contributions to future sea-level rise. In particular, Antarctica's future evolution remains uncertain as mechanisms of dynamic instabilities may arise. Despite having a low probability, these instability mechanisms could lead to the rapid retreat and potential loss of large parts of West Antarctica and thus constitute a high risk for coastal communities.

To support the monitoring of the ice sheets, new satellite missions have been launched—GRACE-FO and ICESat-2 in 2018—and are planned for the future, including the Copernicus Polar Ice and Snow Topography Altimeter (CRISTAL) mission which will embark a dual-frequency radar altimeter and the NASA-ISRO (Indian Space Research Organisation) Synthetic Aperture Radar (NISAR) mission which will be equipped with a dual-frequency SAR instrument. In parallel, new methods and processing schemes to exploit the very large amount of satellite data collected during the past three decades also need to be developed to further our understanding of the processes at play in Greenland and Antarctica. Ensuring the continuity of this invaluable satellite record is key to observe changes occurring across the ice sheets as well as to predict their future evolutions.

Finally, we outline a set of priorities to further improve ice sheet mass balance estimates. First, related to the collection of new measurements to support the calculation of mass balance, it is critical to ensure the continuity of the satellite altimetry record beyond CryoSat-2 and ICESat-2. In addition, it is highly important to remedy the lack of ice thickness measurements in the margins of the ice sheets that currently limit our ability to accurately measure ice discharge by coordinating dedicated airborne campaigns. Second, further reconciling the mass budget method, altimetry, and gravimetry estimates and exploring the remaining biases between these independent techniques will lead to further confidence in our ability to measure changes in the ice sheets, especially in East Antarctica,

where the spread of estimates is high. This can only be achieved by continuing efforts of recent model inter-comparisons of SMB, GIA, and firn compaction models and developing more robust uncertainty characterisation of mass balance estimates. Third, a focus on using this long record of ice sheet mass change to investigate teleconnections with other parts of the climate system and to develop early warning systems of tipping points should be a scientific priority. Last, working closely with the modelling community to ensure that ice sheet mass balance estimates produced by the remote sensing community can effectively be used for calibrating projections of future sea-level rise is essential.

Acknowledgements IO acknowledges support from the UK Natural Environment Research Council Centre for Polar Observation and Modelling (Grant No. cpom300001). SN acknowledges funding support from the NASA Cryosphere and NASA Sea Level Change Programs. The presented data products on gravimetry-based mass change estimates were developed in the framework of the ESA Climate Change Initiative (CCI) projects Antarctic Ice Sheet CCI and CCI+ (Contract Numbers 4000112227/15/I-NB, 4000126813/19/I-NB) and Greenland Ice Sheet CCI and CCI+ (Contract Numbers 4000112228/15/I-NB, 4000126523/19/I-NB).

Declarations

Conflict of interest The authors have no competing interests to declare that are relevant to the content of this article.

Open Access This article is licensed under a Creative Commons Attribution 4.0 International License, which permits use, sharing, adaptation, distribution and reproduction in any medium or format, as long as you give appropriate credit to the original author(s) and the source, provide a link to the Creative Commons licence, and indicate if changes were made. The images or other third party material in this article are included in the article's Creative Commons licence, unless indicated otherwise in a credit line to the material. If material is not included in the article's Creative Commons licence and your intended use is not permitted by statutory regulation or exceeds the permitted use, you will need to obtain permission directly from the copyright holder. To view a copy of this licence, visit <http://creativecommons.org/licenses/by/4.0/>.

References

- Abshire JB, Sun X, Riris H, Sirota JM, McGarry JF, Palm S, Yi D, Liiva P (2005) Geoscience laser altimeter system (GLAS) on the ICESat mission: on-orbit measurement performance. *Geophys Res Lett*. <https://doi.org/10.1029/2005GL024028>
- Adusumilli SA, Fish M, Fricker HA, Medley B (2021) Atmospheric River precipitation contributed to rapid increases in surface height of the west antarctic ice sheet in 2019. *Geophys Res Lett* 48:e2020GL091076. <https://doi.org/10.1029/2020GL091076>
- Agosta C, Amory C, Kittel C, Orsi A, Favier V, Gallée H, van den Broeke MR, Lenaerts JTM, van Wessem JM, van de Berg WJ, Fettweis X (2019) Estimation of the Antarctic surface mass balance using the regional climate model MAR (1979–2015) and identification of dominant processes. *Cryosphere* 13:281–296. <https://doi.org/10.5194/tc-13-281-2019>
- Arndt JE, Schenke HW, Jakobsson M, Nitsche FO, Buys G, Goleby B, Rebesco M, Bohoyo F, Hong J, Black J, Greku R, Udintsev G, Barrios F, Reynoso-Peralta W, Taisei M, Wigley R (2013) The International Bathymetric Chart of the Southern Ocean (IBCSO) version 1.0—a new bathymetric compilation covering circum-Antarctic waters. *Geophys Res Lett* 40:3111–3117. <https://doi.org/10.1002/grl.50413>
- Asay-Davis XS, Cornford SL, Durand G, Galton-Fenzi BK, Gladstone RM, Gudmundsson GH, Hattermann T, Holland DM, Holland D, Holland PR, Martin DF, Mathiot P, Pattyn F, Seroussi H (2016) Experimental design for three interrelated marine ice sheet and ocean model intercomparison projects: MIS-MIP v. 3 (MISMIP +), ISOMIP v. 2 (ISOMIP +) and MISOMIP v. 1 (MISOMIP1). *Geosci Model Dev* 9:2471–2497. <https://doi.org/10.5194/gmd-9-2471-2016>
- Bamber J, Dawson G (2020) Complex evolving patterns of mass loss from Antarctica's largest glacier. *Nat Geosci* 13:127–131. <https://doi.org/10.1038/s41561-019-0527-z>
- Bamber JL, Vaughan DG, Joughin I (2000) Widespread complex flow in the interior of the antarctic ice sheet. *Science* 287:1248–1250. <https://doi.org/10.1126/science.287.5456.1248>

- Banwell AF, MacAyeal DR, Sergienko OV (2013) Breakup of the Larsen B Ice Shelf triggered by chain reaction drainage of supraglacial lakes. *Geophys Res Lett* 40:5872–5876. <https://doi.org/10.1002/2013GL057694>
- Barletta VR, Sørensen LS, Forsberg R (2013) Scatter of mass changes estimates at basin scale for Greenland and Antarctica. *Cryosphere* 7:1411–1432. <https://doi.org/10.5194/tc-7-1411-2013>
- Barletta VR, Bevis M, Smith BE, Wilson T, Brown A, Bordoni A, Willis M, Khan SA, Rovira-Navarro M, Dalziel I, Smalley R, Kendrick E, Konfal S, Caccamise DJ, Aster RC, Nyblade A, Wiens DA (2018) Observed rapid bedrock uplift in Amundsen Sea Embayment promotes ice-sheet stability. *Science* 360:1335–1339. <https://doi.org/10.1126/science.aao1447>
- Barthel A, Agosta C, Little CM, Hattermann T, Jourdain NC, Goelzer H, Nowicki S, Seroussi H, Straneo F, Bracegirdle TJ (2020) CMIP5 model selection for ISMIP6 ice sheet model forcing: Greenland and Antarctica. *Cryosphere* 14:855–879. <https://doi.org/10.5194/tc-14-855-2020>
- Benn DI, Warren CR, Mottram RH (2007) Calving processes and the dynamics of calving glaciers. *Earth Sci Rev* 82:143–179. <https://doi.org/10.1016/j.earscirev.2007.02.002>
- Benn DI, Cowton T, Todd J, Luckman A (2017) Glacier calving in Greenland. *Curr Clim Change Rep* 3:282–290. <https://doi.org/10.1007/s40641-017-0070-1>
- Bennett MR (2003) Ice streams as the arteries of an ice sheet: their mechanics, stability and significance. *Earth Sci Rev* 61:309–339. [https://doi.org/10.1016/S0012-8252\(02\)00130-7](https://doi.org/10.1016/S0012-8252(02)00130-7)
- Berthier E, Scambos TA, Shuman CA (2012) Mass loss of Larsen B tributary glaciers (Antarctic Peninsula) unabated since 2002. *Geophys Res Lett.* <https://doi.org/10.1029/2012GL051755>
- Bettadpur S (2018) UTCSR level-2 processing standards document (for level-2 product release 0006) (Rev. 5.0, April 18, 2018). GRACE Publication, pp 327–742
- Bindschadler RA, Scambos TA (1991) Satellite-Image-derived velocity field of an Antarctic ice stream. *Science* 252:242–246. <https://doi.org/10.1126/science.252.5003.242>
- Böning CW, Behrens E, Biastoch A, Getzlaff K, Bamber JL (2016) Emerging impact of Greenland meltwater on deepwater formation in the North Atlantic Ocean. *Nat Geosci* 9:523–527. <https://doi.org/10.1038/ngeo2740>
- Burton-Johnson A, Dziadek R, Martin C (2020) Review article: geothermal heat flow in Antarctica: current and future directions. *Cryosphere* 14:3843–3873. <https://doi.org/10.5194/tc-14-3843-2020>
- Caesar L, Rahmstorf S, Robinson A, Feulner G, Saba V (2018) Observed fingerprint of a weakening Atlantic Ocean overturning circulation. *Nature* 556:191–196. <https://doi.org/10.1038/s41586-018-0006-5>
- Caron L, Ivins ER, Larour E, Adhikari S, Nilsson J, Blewitt G (2018) GIA model statistics for GRACE hydrology, cryosphere, and ocean science. *Geophys Res Lett* 45:2203–2212. <https://doi.org/10.1016/j.epsl.2019.115957>
- Choi Y, Morlighem M, Rignot E, Wood M (2021) Ice dynamics will remain a primary driver of Greenland ice sheet mass loss over the next century. *Commun Earth Environ.* <https://doi.org/10.1038/s43247-021-00092-z>
- Christianson K, Bushuk M, Dutrieux P, Parizek BR, Joughin IR, Alley RB, Shean DE, Abrahamsen EP, Anandakrishnan S, Heywood KJ, Kim TW, Lee SH, Nicholls K, Stanton T, Truffer M, Webber BGM, Jenkins A, Jacobs S, Bindschadler R, Holland DM (2016) Sensitivity of Pine Island Glacier to observed ocean forcing. *Geophys Res Lett* 43:10817–10825. <https://doi.org/10.1002/2016GL070500>
- Cogley JG, Hock R, Rasmussen LA, Arendt AA, Bauder A, Braithwaite RJ, Jansson R, Kaser G, Möller L, Nicholson L, Zemp M (2011) Glossary of glacier mass balance and related terms. ParisIACS Contribution No. 2
- Dahle C, Murböck M, Flechtner F, Dobslaw H, Michalak G, Neumayer KH, Abrykosov O, Reinhold A, König R, Sulzbach R, Förste C (2019) The GFZ GRACE RL06 monthly gravity field time series: processing details and quality assessment. *Remote Sens* 11(18):2116. <https://doi.org/10.3390/rs11182116>
- Davis PED, Jenkins A, Nicholls KW, Brennan PV, Abrahamsen EP, Heywood KJ, Dutrieux P, Cho KH, Kim TW (2018) Variability in basal melting beneath pine island ice shelf on weekly to monthly time-scales. *J Geophys Res Oceans* 123:8655–8669. <https://doi.org/10.1029/2018JC014464>
- De Angelis H, Skvarca P (2003) Glacier surge after ice shelf collapse. *Science* 299:1560–1562. <https://doi.org/10.1126/science.1077987>
- De Rydt J, Reese R, Paolo FS, Gudmundsson GH (2021) Drivers of Pine Island Glacier speed-up between 1996 and 2016. *Cryosphere* 15:113–132. <https://doi.org/10.5194/tc-15-113-2021>
- de Fleurian B, Morlighem M, Seroussi H, Rignot E, van den Broeke MR, Kuipers Munneke P, Mouginot J, Smeets PCJP, Tedstone AJ (2016) A modeling study of the effect of runoff variability on the effective pressure beneath Russell Glacier, West Greenland. *J Geophys Res Earth Surf* 121:1834–1848. <https://doi.org/10.1002/2016JF003842>

- DeConto RM, Pollard D (2016) Contribution of Antarctica to past and future sea-level rise. *Nature* 531:591–591. <https://doi.org/10.1038/nature17145>
- Delhasse A, Fettweis X, Kittel C, Amory C, Agosta C (2018) Brief communication: Impact of the recent atmospheric circulation change in summer on the future surface mass balance of the Greenland Ice Sheet. *Cryosphere* 12:3409–3418. <https://doi.org/10.5194/tc-12-3409-2018>
- Depoorter MA, Bamber JL, Griggs JA, Lenaerts JTM, Ligtenberg SRM, van den Broeke MR, Moholdt G (2013) Calving fluxes and basal melt rates of Antarctic ice shelves. *Nature* 502:89–92. <https://doi.org/10.1038/nature12567>
- Diener T, Sasgen I, Agosta C, Fürst JJ, Braun MH, Konrad H, Fettweis X (2021) Acceleration of dynamic ice loss in Antarctica from satellite gravimetry. *Front Earth Sci*. <https://doi.org/10.3389/feart.2021.741789>
- Ditmar P (2022) How to quantify the accuracy of mass anomaly time-series based on GRACE data in the absence of knowledge about true signal? *J Geodesy* 96(8):1–22. <https://doi.org/10.1007/s00190-022-01640-x>
- Dobslaw H, Bergmann-Wolf I, Dill R, Poropat L, Thomas M, Dahle C, Esselborn S, König R, Flechtner F (2017) A new high-resolution model of non-tidal atmosphere and ocean mass variability for de-aliasing of satellite gravity observations: AOD1B RL06. *Geophys J Int* 211:263–269. <https://doi.org/10.1093/gji/ggx302>
- Döhne T, Horwath M, Groh A, Buchta E (2023) The sensitivity kernel perspective on GRACE mass change estimates. *J Geodesy*. <https://doi.org/10.1007/s00190-022-01697-8>
- Dupont, T. K., Alley, R. B. (2005) Assessment of the importance of ice-shelf buttressing to ice-sheet flow. *Geophysical research letters*, 32:L04503-n/a. <https://doi.org/10.1029/2004GL022024>
- Dutrieux P, De Rydt J, Jenkins A, Holland PR, Ha HK, Lee SH, Steig EJ, Ding Q, Abrahamsen EP, Schröder M (2014) Strong sensitivity of Pine Island ice-shelf melting to climatic variability. *Science* 343:174–178. <https://doi.org/10.1126/science.1244341>
- Edwards TL, Brandon MA, Durand G, Edwards NR, Golledge NR, Holden PB, Nias IJ, Payne AJ, Ritz C, Wernecke A (2019) Revisiting Antarctic ice loss due to marine ice-cliff instability. *Nature* 566:58–64. <https://doi.org/10.1038/s41586-019-0901-4>
- Edwards TL, Nowicki S, Marzeion B, Hock R, Goelzer H, Seroussi H, Jourdain NC, Slater DA, Turner FE, Smith CJ, McKenna CM, Simon E, Abe-Ouchi A, Gregory JM, Larour E, Lipscomb WH, Payne AJ, Shepherd A, Agosta C, Alexander P, Albrecht T, Anderson B, Asay-Davis X, Aschwanden A, Barthel A, Bliss A, Calov R, Chambers C, Champollion N, Choi Y, Cullather R, Cuzzone J, Dumas C, Felikson D, Fettweis X, Fujita K, Galton-Fenzi BK, Gladstone R, Golledge NR, Greve R, Hattermann T, Hoffman MJ, Humbert A, Huss M, Huybrechts P, Immerzeel W, Kleiner T, Kraaijenbrink P, Le clec’h, S., Lee, V., Leguy, G. R., Little, C. M., Lowry, D. P., Malles, J.-H., Martin, D. F., Maussion, F., Morlighem, M., O’Neill, J. F., Nias, I., Pattyn, F., Pelle, T., Price, S. F., Quiquet, A., Radić, V., Reese, R., Rounce, D. R., Rückamp, M., Sakai, A., Shafer, C., Schlegel, N.-J., Shannon, S., Smith, R. S., Straneo, F., Sun, S., Tarasov, L., Trusel, L. D., Van Breedam, J., van de Wal, R., van den Broeke, M., Winkelmann, R., Zekollari, H., Zhao, C., Zhang, T., Zwinger, T. (2021) Projected land ice contributions to twenty-first-century sea level rise. *Nature* 593:74–82. <https://doi.org/10.1038/s41586-021-03302-y>
- Enderlin EM, Howat IM, Jeong S, Noh MJ, Angelen JH, van den Broeke MR (2014) An improved mass budget for the Greenland ice sheet. *Geophys Res Lett* 41:866–872. <https://doi.org/10.1002/2013GL059010>
- Engels O, Gunter B, Riva R, Klees R (2018) Separating geophysical signals using GRACE and high-resolution data: a case study in Antarctica. *Geophysical Res Lett* 45:12340–312349. <https://doi.org/10.1029/2018GL079670>
- Ettema J, van den Broeke MR, van Meijgaard E, van de Berg WJ (2010) Climate of the Greenland ice sheet using a high-resolution climate model—part 2: near-surface climate and energy balance. *Cryosphere* 4:529–544. <https://doi.org/10.5194/tc-4-529-2010>
- Farinotti D, Huss M, Fürst JJ, Landmann J, Machguth H, Maussion F, Pandit A (2019) A consensus estimate for the ice thickness distribution of all glaciers on Earth. *Nat Geosci* 12:168–173. <https://doi.org/10.1038/s41561-019-0300-3>
- Farrell WE, Clark JA (1976) On postglacial sea level. *Geophys J Int* 46:647–667. <https://doi.org/10.1111/j.1365-246X.1976.tb01252.x>
- Fausto RS, Box JE, Vandecrux B, Van As D, Steffen K, Macferrin MJ, Machguth H, Colgan W, Koenig LS, McGrath D, Charalampidis C, Braithwaite RJ (2018) A snow density dataset for improving surface boundary conditions in Greenland ice sheet firn modeling. *Front Earth Sci*. <https://doi.org/10.3929/ethz-b-000268508>

- Felikson D, Urban TJ, Gunter BC, Pie N, Pritchard HD, Harpold R, Schutz BE (2017) Comparison of elevation change detection methods from ICESat altimetry over the Greenland ice sheet. *IEEE Trans Geosci Remote Sens* 55:5494–5505. <https://doi.org/10.1109/TGRS.2017.2709303>
- Fettweis X, Box JE, Agosta C, Amory C, Kittel C, Lang C, van As D, Machguth H, Gallée H (2017) Reconstructions of the 1900–2015 Greenland ice sheet surface mass balance using the regional climate MAR model. *Cryosphere* 11:1015–1033. <https://doi.org/10.5194/tc-11-1015-2017>
- Fettweis X, Hofer S, Krebs-Kanzow U, Amory C, Aoki T, Berends CJ, Born A, Box JE, Delhasse A, Fujita K, Gierz P, Goelzer H, Hanna E, Hashimoto A, Huybrechts P, Kapsch ML, King MD, Kittel C, Lang C, Langen PL, Lenaerts JTM, Liston GE, Lohmann G, Mernild SH, Mikolajewicz U, Modali K, Mottram RH, Niwano M, Noël B, Ryan JC, Smith A, Streffing J, Tedesco M, van de Berg WJ, van den Broeke M, van de Wal RSW, van Kampenhout L, Wilton D, Wouters B, Ziemen F, Zolles T (2020) GrSMBMIP: intercomparison of the modelled 1980–2012 surface mass balance over the Greenland Ice Sheet. *Cryosphere* 14:3935–3958. <https://doi.org/10.5194/tc-14-3935-2020>
- Flament T, Rémy F (2012) Dynamic thinning of Antarctic glaciers from along-track repeat radar altimetry. *J Glaciol* 58:830–840. <https://doi.org/10.3189/2012JG011118>
- Forsberg R, Sørensen L, Simonsen S (2017) Greenland and Antarctica ice sheet mass changes and effects on global sea level. *Surv Geophys* 38:89–104. <https://doi.org/10.1007/s10712-016-9398-7>
- Fox Maule CF, Purucker ME, Olsen N, Mosegaard K (2005) Heat flux anomalies in Antarctica revealed by satellite magnetic data. *Science* 309:464–467. <https://doi.org/10.1126/science.1106888>
- Fox-Kemper B, Hewitt HT, Xiao C, Aðalgeirsdóttir G, Drijfhout SS, Edwards TL, Golledge NR, Hemer M, Kopp RE, Krinner G, Mix A, Notz D, Nowicki S, Nurhati IS, Ruiz L, Sallée J-B, Slangen ABA, Yu Y (2021) Ocean, cryosphere and sea level change. Cambridge University Press, Cambridge
- Fretwell P, Pritchard HD, Vaughan DG, Bamber JL, Barrand NE, Bell R, Bianchi C, Bingham RG, Blankenship DD, Casassa G, Catania G, Callens D, Conway H, Cook AJ, Corr HFJ, Damaske D, Damm V, Ferraccioli F, Forsberg R, Fujita S, Gim Y, Gogineni P, Griggs JA, Hindmarsh RCA, Holmlund P, Holt JW, Jacobel RW, Jenkins A, Jokat W, Jordan T, King EC, Kohler J, Krabill W, Riger-Kusk M, Langley KA, Leitchenkov G, Leuschen C, Luyendyk BP, Matsuoka K, Mouginot J, Nitsche FO, Nogi Y, Nost OA, Popov SV, Rignot E, Ripplin DM, Rivera A, Roberts J, Ross N, Siegert MJ, Smith AM, Steinhage D, Studinger M, Sun B, Tinto BK, Welch BC, Wilson D, Young DA, Xiangbin C, Zirizzotti A (2013) Bedmap2: improved ice bed, surface and thickness datasets for Antarctica. *Cryosphere* 7:375–393. <https://doi.org/10.5194/tc-7-375-2013>
- Fricker HA, Coleman R, Padman L, Scambos TA, Bohlander J, Brunt KM (2009) Mapping the grounding zone of the Amery Ice Shelf, East Antarctica using InSAR, MODIS and ICESat. *Antarct Sci* 21:515–532. <https://doi.org/10.1017/S095410200999023X>
- Fyke J, Sergienko O, Löfverström M, Price S, Lenaerts JTM (2018) An overview of interactions and feedbacks between ice sheets and the earth system. *Rev Geophys* 56:361–408. <https://doi.org/10.1029/2018RG000600>
- Gardner AS, Moholdt G, Scambos T, Fahnestock M, Ligtenberg S, van den Broeke M, Nilsson J (2018) Increased West Antarctic and unchanged East Antarctic ice discharge over the last 7 years. *Cryosphere* 12:521–547. <https://doi.org/10.5194/tc-12-521-2018>
- Gillet-Chaulet F, Gagliardini O, Seddik H, Nodet M, Durand G, Ritz C, Zwinger T, Greve R, Vaughan DG (2012) Greenland ice sheet contribution to sea-level rise from a new-generation ice-sheet model. *Cryosphere* 6:1561–1576
- Goelzer H, Robinson A, Seroussi H, van de Wal RSW (2017) Recent progress in Greenland ice sheet modelling. *Curr Clim Change Rep* 3:291–302. <https://doi.org/10.1007/s40641-017-0073-y>
- Goelzer H, Nowicki S, Payne A, Larour E, Seroussi H, Lipscomb WH, Gregory J, Abe-Ouchi A, Shepherd A, Simon E, Agosta C, Alexander P, Aschwanden A, Barthel A, Calov R, Chambers C, Choi Y, Cuzzone J, Dumas C, Edwards T, Felikson D, Fettweis X, Golledge NR, Greve R, Humbert A, Huybrechts P, Le clec'h, S., Lee, V., Leguy, G., LITTLE, C., Lowry, D. P., Morlighem, M., Nias, I., Quiquet, A., Rückamp, M., Schlegel, N. J., Slater, D. A., Smith, R. S., Straneo, F., Tarasov, L., van de Wal, R., van den Broeke, M. (2020) The future sea-level contribution of the Greenland ice sheet: a multi-model ensemble study of ISMIP6. *Cryosphere* 14:3071–3096. <https://doi.org/10.5194/tc-14-3071-2020>
- Golledge NR, Keller ED, Gomez N, Naughten KA, Bernaldes J, Trusel LD, Edwards TL (2019) Global environmental consequences of twenty-first-century ice-sheet melt. *Nature* 566:65–72. <https://doi.org/10.1038/s41586-019-0889-9>
- Gomez N, Mitrovica JX, Huybers P, Clark PU (2010) Sea level as a stabilizing factor for marine-ice-sheet grounding lines. *Nat Geosci* 3:850–853. <https://doi.org/10.1038/ngeo1012>
- Groh A, Horwath M (2021) Antarctic ice mass change products from GRACE/GRACE-FO using tailored sensitivity kernels. *Remote Sens* 13:1736. <https://doi.org/10.3390/rs13091736>

- Groh A, Horwath M, Horvath A, Meister R, Sørensen LS, Barletta VR, Forsberg R, Wouters B, Ditmar P, Ran J, Klees R, Su X, Shang K, Guo J, Shum CK, Schrama E, Shepherd A (2019) Evaluating GRACE mass change time series for the Antarctic and Greenland ice sheet—methods and results. *Geosciences* 9:21. <https://doi.org/10.3390/geosciences9100415>
- Gudmundsson GH, Paolo FS, Adusumilli S, Fricker HA (2019) Instantaneous Antarctic ice sheet mass loss driven by thinning ice shelves. *Geophys Res Lett* 46:13903–13909. <https://doi.org/10.1029/2019GL085027>
- Haagmans R, Siemes C, Massotti L, Carraz O, Silvestrin P (2020) ESA's next-generation gravity mission concepts, *Rendiconti Lincei. Scienze Fisiche e Naturali* 31:15–25. <https://doi.org/10.1007/s12210-020-00875-0>
- Hanna E, Cappelen J, Fettweis X, Mernild SH, Mote TL, Mottram R, Steffen K, Ballinger TJ, Hall RJ (2020) Greenland surface air temperature changes from 1981 to 2019 and implications for ice-sheet melt and mass-balance change. *Int J Climatol* 41:E1336–E1352. <https://doi.org/10.1002/joc.6771>
- Hogg AE, Shepherd A, Gilbert L, Muir A, Drinkwater MR (2018) Mapping ice sheet grounding lines with CryoSat-2. *Adv Space Res* 62:1191–1202. <https://doi.org/10.1016/j.asr.2017.03.008>
- Holland DM, Thomas RH, de Young B, Ribergaard MH, Lyberth B (2008) Acceleration of Jakobshavn Isbræ triggered by warm subsurface ocean waters. *Nat Geosci* 1:659–664. <https://doi.org/10.1038/ngeo316>
- Horwath M, Dietrich R (2009) Signal and error in mass change inferences from GRACE: the case of Antarctica. *Geophys J Int* 177:849–864. <https://doi.org/10.1111/j.1365-246X.2009.04139.x>
- Horwath M, Legrésy B, Rémy F, Blarel F, Lemoine JM (2012) Consistent patterns of Antarctic ice sheet interannual variations from ENVISAT radar altimetry and GRACE satellite gravimetry. *Geophys J Int* 189:863–876. <https://doi.org/10.1111/j.1365-246X.2012.05401.x>
- Howat IM, Eddy A (2011) Multi-decadal retreat of Greenland's marine-terminating glaciers. *J Glaciol* 57:389–396. <https://doi.org/10.3189/002214311796905631>
- Howat IM, Porter C, Smith BE, Noh MJ, Morin P (2019) The reference elevation model of Antarctica. *Cryosphere* 13:665–674. <https://doi.org/10.5194/tc-13-665-2019>
- Howat I, Negrete A, Smith B (2015) MEaSUREs Greenland Ice mapping project (GIMP) digital elevation model, Version 1. NASA National Snow and Ice Data Center Distributed Active Archive Center, Boulder, Colorado USA
- Hsu C-W, Velicogna I (2017) Detection of sea level fingerprints derived from GRACE gravity data. *Geophys Res Lett* 44:8953–8961. <https://doi.org/10.1002/2017GL074070>
- Jäggi A, Meyer U, Lasser M, et al (2020) International combination service for time-variable gravity fields (COST-G). In: *International association of geodesy symposia*. Springer Berlin, Heidelberg
- Jenkins A (2011) Convection-driven melting near the grounding lines of ice shelves and tidewater glaciers. *J Phys Oceanogr* 41:2279–2294. <https://doi.org/10.1175/JPO-D-11-03.1>
- Joughin I (2002) Ice-sheet velocity mapping: a combined interferometric and speckle-tracking approach. *Ann Glaciol* 34:195–201. <https://doi.org/10.3189/172756402781817978>
- Joughin I, Howat IM, Fahnestock M, Smith B, Krabill W, Alley RB, Stern H, Truffer M (2008) Continued evolution of Jakobshavn Isbræ following its rapid speedup. *J Geophys Res Earth Surf*. <https://doi.org/10.1029/2008JF001023>
- Joughin I, Alley RB, Holland DM (2012) Ice-sheet response to oceanic forcing. *Science* 338:1172–1176. <https://doi.org/10.1126/science.1226481>
- Joughin I, Smith BE, Medley B (2014a) Marine ice sheet collapse potentially under way for the Thwaites Glacier Basin, West Antarctica. *Science* 344:735–738. <https://doi.org/10.1126/science.1249055>
- Joughin I, Smith BE, Shean DE, Floricioiu D (2014b) Brief communication: further summer speedup of Jakobshavn Isbræ. *Cryosphere* 8:209–214. <https://doi.org/10.5194/tc-8-209-2014>
- Joughin I, Shean DE, Smith BE, Dutrieux P (2016) Grounding line variability and subglacial lake drainage on Pine Island Glacier, Antarctica. *Geophys Res Lett* 43:9093–9102. <https://doi.org/10.1002/2016GL070259>
- Joughin I, Smith B, Howat I, Scambos T (2010) MEaSUREs Greenland ice sheet velocity map from InSAR Data, Version 1. Boulder, Colorado USA. NASA National Snow and Ice Data Center Distributed Active Archive Center
- Jourdain NC, Asay-Davis X, Hattermann T, Straneo F, Seroussi H, Little CM, Nowicki S (2020) A protocol for calculating basal melt rates in the ISMIP6 Antarctic ice sheet projections. *Cryosphere* 14:3111–3134. <https://doi.org/10.5194/tc-14-3111-2020>
- Kappelsberger MT, Ströbenreuther U, Scheinert M, Horwath M, Groh A, Knöfel C, Lunz S, Khan SA (2021) Modeled and observed bedrock displacements in North-East Greenland using refined estimates of present-day ice-mass changes and densified GNSS measurements. *J Geophys Res Earth Surf* 126:e2020JF005860. <https://doi.org/10.1029/2020JF005860>

- Karlsson NB, Solgaard AM, Mankoff KD, Gillet-Chaulet F, MacGregor JA, Box JE, Citterio M, Colgan WT, Larsen SH, Kjeldsen KK, Korsgaard NJ, Benn DI, Hewitt IJ, Fausto RS (2021) A first constraint on basal melt-water production of the Greenland ice sheet. *Nat Commun* 12:3461. <https://doi.org/10.1038/s41467-021-23739-z>
- Khazendar A, Rignot E, Schroeder DM, Seroussi H, Schodlok MP, Scheuchl B, Mouginot J, Sutterley TC, Velicogna I (2016) Rapid submarine ice melting in the grounding zones of ice shelves in West Antarctica. *Nat Commun* 7:13243. <https://doi.org/10.1038/ncomms13243>
- Khazendar A, Fenty IG, Carroll D, Gardner A, Lee CM, Fukumori I, Wang O, Zhang H, Seroussi H, Moller D, Noël BPY, van den Broeke MR, Dinardo S, Willis J (2019) Interruption of two decades of Jakobshavn Isbrae acceleration and thinning as regional ocean cools. *Nat Geosci* 12:277–283. <https://doi.org/10.1038/s41561-019-0329-3>
- King MD, Howat IM, Jeong S, Noh MJ, Wouters B, Noël B, van den Broeke MR (2018) Seasonal to decadal variability in ice discharge from the Greenland Ice Sheet. *Cryosphere* 12:3813–3825. <https://doi.org/10.5194/tc-12-3813-2018>
- King MD, Howat IM, Candela SG, Noh MJ, Jeong S, Noël BPY, van den Broeke MR, Wouters B, Negrete A (2020) Dynamic ice loss from the Greenland Ice Sheet driven by sustained glacier retreat. *Commun Earth Environ* 1:1. <https://doi.org/10.1038/s43247-020-0001-2>
- Koenig LS, Ivanoff A, Alexander PM, MacGregor JA, Fettweis X, Panzer B, Paden JD, Forster RR, Das I, McConnell JR, Tedesco M, Leuschen C (2016) Annual Greenland accumulation rates (2009–2012) from airborne snow radar. <https://doi.org/10.7916/D8X07KHT>
- Konrad H, Sasgen I, Pollard D, Klemann V (2015) Potential of the solid-Earth response for limiting long-term West Antarctic Ice Sheet retreat in a warming climate. *Earth Planet Sci Lett* 432:254–264. <https://doi.org/10.1016/j.epsl.2015.10.008>
- Konrad H, Gilbert L, Cornford SL, Payne A, Hogg A, Muir A, Shepherd A (2017) Uneven onset and pace of ice-dynamical imbalance in the Amundsen Sea Embayment, West Antarctica: drawdown in the Amundsen Sea Embayment. *Geophys Res Lett* 44:910–918. <https://doi.org/10.1002/2016GL070733>
- Kuipers Munneke P, Ligtenberg SRM, Noël BPY, Howat IM, Box JE, Mosley-Thompson E, McConnell JR, Steffen K, Harper JT, Das SB, van den Broeke MR (2015) Elevation change of the Greenland Ice Sheet due to surface mass balance and firn processes, 1960–2014. *Cryosphere* 9:2009–2025. <https://doi.org/10.5194/tc-9-2009-2015>
- Kulp SA, Strauss BH (2019) New elevation data triple estimates of global vulnerability to sea-level rise and coastal flooding. *Nat Commun* 10:4844. <https://doi.org/10.1038/s41467-019-12808-z>
- Kusche J, Schmidt R, Petrovic S, Rietbroek R (2009) Decorrelated GRACE time-variable gravity solutions by GFZ, and their validation using a hydrological model. *J Geodesy* 83:903–913. <https://doi.org/10.1007/s00190-009-0308-3>
- Kvas A, Behzadpour S, Ellmer M, Klinger B, Strasser S, Zehentner N, Mayer-Gürr T (2019) ITSG-Grace2018: overview and evaluation of a new GRACE-only gravity field time series. *J Geophys Res Solid Earth*. <https://doi.org/10.1029/2019JB017415>
- Landerer FW, Flechtner FM, Save H, Webb FH, Bandikova T, Bertiger WI, Bettadpur SV, Byun SH, Dahle C, Dobslaw H, Fahnestock E, Harvey N, Kang Z, Kruizinga GLH, Loomis BD, McCullough C, Murböck M, Nagel P, Paik M, Pie N, Poole S, Strelakov D, Tamisiea ME, Wang F, Watkins MM, Wen HY, Wiese DN, Yuan DN (2020) Extending the global mass change data record: GRACE follow-on instrument and science data performance. *Geophys Res Lett* 47:e2020G088306. <https://doi.org/10.1029/2020GL088306>
- Langen PL, Fausto RS, Vandecrux B, Mottram RH, Box JE (2017) Liquid water flow and retention on the Greenland ice sheet in the regional climate model HIRHAM5: local and large-scale impacts. *Front Earth Sci*. <https://doi.org/10.3389/feart.2016.00110>
- Larour E, Morlighem M, Seroussi H, Schiermeier J, Rignot E (2012) Ice flow sensitivity to geothermal heat flux of Pine Island Glacier, Antarctica. *J Geophys Res Earth Surf*. <https://doi.org/10.1029/2012JF002371>
- Larour E, Seroussi H, Adhikari S, Ivins E, Caron L, Morlighem M, Schlegel N (2019) Slowdown in Antarctic mass loss from solid Earth and sea-level feedbacks. *Science* 364:eav7908. <https://doi.org/10.1126/science.aav7908>
- Le Brocq AM, Ross N, Griggs JA, Bingham RG, Corr HFJ, Ferraccioli F, Jenkins A, Jordan TA, Payne AJ, Rippin DM, Siegert MJ (2013) Evidence from ice shelves for channelized meltwater flow beneath the Antarctic Ice Sheet. *Nat Geosci* 6:945–948. <https://doi.org/10.1038/ngeo1977>
- Leeson AA, Shepherd A, Briggs K, Howat I, Fettweis X, Morlighem M, Rignot E (2015) Supraglacial lakes on the Greenland ice sheet advance inland under warming climate. *Nat Clim Chang* 5:51–55. <https://doi.org/10.1038/nclimate2463>

- Lenaerts JTM, Medley B, Broeke MR, Wouters B (2019) Observing and modeling ice sheet surface mass balance. *Rev Geophys* 57:376–420. <https://doi.org/10.1029/2018RG000622>
- Levermann A, Winkelmann R, Albrecht T, Goelzer H, Golledge NR, Greve R, Huybrechts P, Jordan J, Leguy G, Martin D, Morlighem M, Pattyn F, Pollard D, Quiquet A, Rodehacke C, Seroussi H, Sutter J, Zhang T, Van Breedam J, Calov R, DeConto R, Dumas C, Garbe J, Gudmundsson GH, Hoffman MJ, Humbert A, Kleiner T, Lipscomb WH, Meinshausen M, Ng E, Nowicki SMJ, Perego M, Price SF, Saito F, Schlegel NJ, Sun S, van de Wal RSW (2020) Projecting Antarctica's contribution to future sea level rise from basal ice shelf melt using linear response functions of 16 ice sheet models (LARMIP-2). *Earth Syst Dyn* 11:35–76. <https://doi.org/10.5194/esd-11-35-2020>
- Lhermitte S, Sun S, Shuman C, Wouters B, Pattyn F, Wuite J, Berthier E, Nagler T (2020) Damage accelerates ice shelf instability and mass loss in Amundsen Sea Embayment. *Proc Natl Acad Sci* 117:24735–24741. <https://doi.org/10.1073/pnas.1912890117>
- Ligtenberg SRM, Kuipers Munneke P, van den Broeke MR (2014) Present and future variations in Antarctic firm air content. *Cryosphere* 8:1711–1723. <https://doi.org/10.5194/tc-8-1711-2014>
- Loomis BD, Luthcke SB, Sabaka TJ (2019a) Regularization and error characterization of GRACE mascons. *J Geodesy* 93:1381–1398. <https://doi.org/10.1007/s00190-019-01252-y>
- Loomis BD, Rachlin KE, Luthcke SB (2019b) Improved earth oblateness rate reveals increased ice sheet losses and mass-driven sea level rise. *Geophys Res Lett* 46:6910–6917. <https://doi.org/10.1029/2019GL082929>
- Lucas-Picher P, Wulff-Nielsen M, Christensen JH, Aðalgeirsdóttir G, Mottram R, Simonsen SB (2012) Very high resolution regional climate model simulations over Greenland: identifying added value. *J Geophys Res Atmosp*. <https://doi.org/10.1029/2011JD016267>
- Luthcke SB, Sabaka TJ, Loomis BD, Arendt AA, McCarthy JJ, Camp J (2013) Antarctica, Greenland and Gulf of Alaska land ice evolution from an iterated GRACE global mascon solution. *J Glac* 59(216):613–631. <https://doi.org/10.3189/2013jJoG12j147>
- MacFerrin M, Machguth H, As DV, Charalampidis C, Stevens CM, Heilig A, Vandecrux B, Langen PL, Mottram R, Fettweis X, Broeke MRVD, Pfeffer WT, Moussavi MS, Abdalati W (2019) Rapid expansion of Greenland's low-permeability ice slabs. *Nature* 573:403–407. <https://doi.org/10.1038/s41586-019-1550-3>
- MacGregor JA, Fahnestock MA, Catania GA, Aschwanden A, Clow GD, Colgan WT, Gogineni SP, Morlighem M, Nowicki SMJ, Paden JD, Price SF, Seroussi H (2016) A synthesis of the basal thermal state of the Greenland Ice Sheet. *J Geophys Res Earth Surf* 121:1328–1350. <https://doi.org/10.1002/2015JF003803>
- Machguth H, MacFerrin M, van As D, Box JE, Charalampidis C, Colgan W, Fausto RS, Meijer HAJ, Mosley-Thompson E, van de Wal RSW (2016) Greenland meltwater storage in firm limited by near-surface ice formation. *Nat Clim Chang* 6:390. <https://doi.org/10.1038/nclimate2899>
- Mankoff KD, Tulaczyk SM (2017) The past, present, and future viscous heat dissipation available for Greenland subglacial conduit formation. *Cryosphere* 11:303–317. <https://doi.org/10.5194/tc-11-303-2017>
- Mankoff KD, Solgaard A, Colgan W, Ahlstrøm AP, Khan SA, Fausto RS (2020) Greenland Ice Sheet solid ice discharge from 1986 through March 2020. *Earth Syst Sci Data* 12:1367–1383. <https://doi.org/10.5194/essd-12-1367-2020>
- Mankoff KD, Fettweis X, Langen PL, Stendel M, Kjeldsen KK, Karlsson NB, Noël B, van den Broeke MR, Solgaard A, Colgan W, Box JE, Simonsen SB, King MD, Ahlstrøm AP, Andersen SB, Fausto RS (2021) Greenland ice sheet mass balance from 1840 through next week. *Earth Syst Sci Data* 13:5001–5025. <https://doi.org/10.5194/essd-13-5001-2021>
- Markus T, Neumann T, Martino A, Abdalati W, Brunt K, Csatho B, Farrell S, Fricker H, Gardner A, Harding D, Jasinski M, Kwok R, Magruder L, Lubin D, Luthcke S, Morison J, Nelson R, Neuen-schwander A, Palm S, Popescu S, Shum C, Schutz BE, Smith B, Yang Y, Zwally J (2017) The Ice, Cloud, and land Elevation Satellite-2 (ICESat-2): science requirements, concept, and implementation. *Remote Sens Environ* 190:260–273. <https://doi.org/10.1016/j.rse.2016.12.029>
- Masson-Delmotte V, Zhai P, Pörtner H-O, Roberts D, Skea J, Shukla PR, Pirani A, Moufouma-Okia W, Péan C, Pidcock R, Connors S, Matthews JBR, Chen Y, Zhou X, Gomis MI, Lonnoy E, Maycock T, Tignor M, Waterfield T (2018) Global Warming of 1.5°C. An IPCC Special Report on the impacts of global warming of 1.5°C above pre-industrial levels and related global greenhouse gas emission pathways, in the context of strengthening the global response to the threat of climate change, sustainable development, and efforts to eradicate poverty. Intergovernmental Panel on Climate Change
- Mattingly KS, Mote TL, Fettweis X (2018) Atmospheric river impacts on Greenland ice sheet surface mass balance. *J Geophys Res Atmosp* 123:8538–8560. <https://doi.org/10.1029/2018JD028714>

- McMillan M, Leeson A, Shepherd A, Briggs K, Armitage TWK, Hogg A, Kuipers Munneke P, van den Broeke M, Noël B, van de Berg WJ, Ligtenberg S, Horwath M, Groh A, Muir A, Gilbert L (2016) A high-resolution record of Greenland mass balance: high-resolution Greenland mass balance. *Geophys Res Lett* 43:7002–7010. <https://doi.org/10.1002/2016GL069666>
- Medley B, Thomas ER (2019) Increased snowfall over the Antarctic Ice Sheet mitigated twentieth-century sea-level rise. *Nat Clim Chang* 9:34–39. <https://doi.org/10.1038/s41558-018-0356-x>
- Mercer JH (1978) West Antarctic ice sheet and CO₂ greenhouse effect: a threat of disaster. *Nature* 271:321–325. <https://doi.org/10.1038/271321a0>
- Meredith M, Sommerkorn M, Cassotta S, Derksen C, Ekaykin A, Hollowed A, Kofinas G, Mackintosh A, Melbourne-Thomas J, Muelbert MMC, Ottersen G, Pritchard H, Schuur EAG (2019) Polar regions. In: IPCC Special Report on the Ocean and Cryosphere in a Changing Climate, Intergovernmental Panel on Climate Change
- Moon T, Joughin I, Smith B, Howat I (2012) 21st-century evolution of Greenland outlet glacier velocities. *Science* 336:576–578. <https://doi.org/10.1126/science.1219985>
- Morlighem M, Seroussi H, Larour E, Rignot E (2013) Inversion of basal friction in Antarctica using exact and incomplete adjoints of a higher-order model. *J Geophys Res Earth Surf* 118:1746–1753. <https://doi.org/10.1002/jgrf.20125>
- Morlighem M, Williams CN, Rignot E, An L, Arndt JE, Bamber JL, Catania G, Chauché N, Dowdeswell JA, Dorschel B, Fenty I, Hogan K, Howat I, Hubbard A, Jakobsson M, Jordan TM, Kjeldsen KK, Millan R, Mayer L, Mouginot J, Noël BPY, O’Cofaigh C, Palmer S, Rysgaard S, Seroussi H, Siegert MJ, Slabon P, Straneo F, van den Broeke MR, Weinrebe W, Wood M, Zinglens KB (2017) BedMachine v3: complete bed topography and ocean bathymetry mapping of Greenland From Multibeam Echo Sounding combined with mass conservation. *Geophys Res Lett* 44:11051–11061. <https://doi.org/10.1002/2017gl074954>
- Morlighem M, Rignot E, Binder T, Blankenship D, Drews R, Eagles G, Eisen O, Ferraccioli F, Forsberg R, Fretwell P, Goel V, Greenbaum JS, Gudmundsson H, Guo J, Helm V, Hofstede C, Howat I, Humbert A, Jokat W, Karlsson NB, Lee WS, Matsuoka K, Millan R, Mouginot J, Paden J, Pattyn F, Roberts J, Rosier S, Ruppel A, Seroussi H, Smith EC, Steinhage D, Sun B, Broeke MR, v. d., Ommen, T. D. v., Wessem, M. v., Young, D. A. (2020) Deep glacial troughs and stabilizing ridges unveiled beneath the margins of the Antarctic ice sheet. *Nat Geosci* 13:132–137. <https://doi.org/10.1038/s41561-019-0510-8>
- Mote TL (2007) Greenland surface melt trends 1973–2007: evidence of a large increase in 2007. *Geophys Res Lett*. <https://doi.org/10.1029/2007GL031976>
- Mottram RB, Simonsen S, Hoyer Svendsen S, Barletta VR, Sandberg Sørensen L, Nagler T, Wuite J, Groh A, Horwath M, Rosier J, Solgaard A, Hvidberg CS, Forsberg R (2019) An integrated view of Greenland Ice Sheet mass changes based on models and satellite observations. *Remote Sens* 11:1407. <https://doi.org/10.3390/rs11121407>
- Mottram R, Hansen N, Kittel C, van Wessem JM, Agosta C, Amory C, Boberg F, van de Berg WJ, Fettweis X, Gossart A, van Lipzig NPM, van Meijgaard E, Orr A, Phillips T, Webster S, Simonsen SB, Souverijns N (2021) What is the surface mass balance of Antarctica? An intercomparison of regional climate model estimates. *Cryosphere* 15:3751–3784. <https://doi.org/10.5194/tc-15-3751-2021>
- Mouginot J, Rignot E, Scheuchl B (2014) Sustained increase in ice discharge from the Amundsen Sea Embayment, West Antarctica, from 1973 to 2013. *Geophys Res Lett* 41:1576–1584. <https://doi.org/10.1002/2013GL059069>
- Mouginot J, Rignot E, Björk AA, van den Broeke M, Millan R, Morlighem M, Noël B, Scheuchl B, Wood M (2019a) Forty-six years of Greenland Ice Sheet mass balance from 1972 to 2018. *Proc Natl Acad Sci* 116:9239–9244. <https://doi.org/10.1073/pnas.1904242116>
- Mouginot J, Rignot E, Scheuchl B (2019b) Continent-wide, interferometric SAR phase, mapping of Antarctic ice velocity. *Geophys Res Lett* 46:9710–9718. <https://doi.org/10.1029/2019GL083826>
- Nerem RS, Beckley BD, Fasullo JT, Hamlington BD, Masters D, Mitchum GT (2018) Climate-change-driven accelerated sea-level rise detected in the altimeter era. *Proc Natl Acad Sci* 115:2022–2025. <https://doi.org/10.1073/pnas.1717312115>
- Nilsson J, Vallengaard P, Simonsen SB, Sørensen LS, Forsberg R, Dahl-Jensen D, Hirabayashi M, Goto-Azuma K, Hvidberg CS, Kjaer HA, Satow K (2015) Greenland 2012 melt event effects on CryoSat-2 radar altimetry: effect of Greenland melt on cryosat-2. *Geophys Res Lett* 42:3919–3926. <https://doi.org/10.1002/2015GL063296>
- Noël B, van de Berg WJ, van Wessem JM, van Meijgaard E, van As D, Lenaerts JTM, Lhermitte S, Kuipers Munneke P, Smeets CJPP, van Ulft LH, van de Wal RSW, van den Broeke MR (2018) Modelling the climate and surface mass balance of polar ice sheets using RACMO2—part 1: Greenland (1958–2016). *Cryosphere* 12:811–831. <https://doi.org/10.5194/tc-12-811-2018>

- Noël B, van Kampenhout L, Lenaerts JTM, van de Berg WJ, van den Broeke MR (2021) A 21st century warming threshold for sustained Greenland Ice sheet mass loss. *Geophys Res Lett* 48:e2020GL090471. <https://doi.org/10.1029/2020GL090471>
- Nowicki S, Seroussi H (2018) Projections of future sea level contributions from the Greenland and Antarctic Ice Sheets: challenges beyond dynamical ice sheet modeling. *Oceanography* 31:8. <https://doi.org/10.5670/oceanog.2018.216>
- Nowicki SMJ, Payne A, Larour E, Seroussi H, Goelzer H, Lipscomb W, Gregory J, Abe-Ouchi A, Shepherd A (2016) Ice sheet model intercomparison project (ISMIP6) contribution to CMIP6. *Geosci Model Dev* 9:4521–4545. <https://doi.org/10.5194/gmd-9-4521-2016>
- Nowicki S, Goelzer H, Seroussi H, Payne AJ, Lipscomb WH, Abe-Ouchi A, Agosta C, Alexander P, Asay-Davis XS, Barthel A, Bracegirdle TJ, Cullather R, Felikson D, Fettweis X, Gregory JM, Hattermann T, Jourdain NC, Kuipers Munneke P, Larour E, Little CM, Morlighem M, Nias I, Shepherd A, Simon E, Slater D, Smith RS, Straneo F, Trusel LD, van den Broeke MR, van de Wal R (2020) Experimental protocol for sea level projections from ISMIP6 stand-alone ice sheet models. *Cryosphere* 14:2331–2368. <https://doi.org/10.5194/tc-14-2331-2020>
- Otosaka I, Shepherd A, McMillan M (2019) Ice sheet elevation change in West Antarctica from Ka-band satellite radar altimetry. *Geophys Res Lett* 6:13135–13143. <https://doi.org/10.1029/2019GL084271>
- Otosaka IN, Shepherd A, Casal TGD, Coccia A, Davidson M, Di Bella A, Fettweis X, Forsberg R, Helm V, Hogg AE, Hvidegaard SM, Lemos A, Macedo K, Kuipers Munneke P, Parrinello T, Simonsen SB, Skourup H, Sørensen LS (2020) Surface melting drives fluctuations in airborne radar penetration in West Central Greenland. *Geophys Res Lett* 47:e2020GL088293. <https://doi.org/10.1029/2020gl088293>
- Otosaka IN, Shepherd A, Ivins ER, Schlegel N-J, Amory C, van den Broeke MR, Horwath M, Joughin I, King MD, Krinner G, Nowicki S, Payne AJ, Rignot E, Scambos T, Simon KM, Smith BE, Sørensen LS, Velicogna I, Whitehouse PL, Agosta C, Ahlstrøm AP, Blazquez A, Colgan W, Engdahl ME, Fettweis X, Forsberg R, Gallée H, Gardner A, Gilbert L, Gourmelen N, Groh A, Gunter BC, Harig C, Helm V, Khan SA, Kittel C, Konrad H, Langen PL, Lecavalier BS, Liang C-C, Loomis BD, McMillan M, Melini D, Mernild SH, Mottram R, Mougnot J, Nilsson J, Noël B, Pattie ME, Peltier WR, Pie N, Roca M, Sasgen I, Save HV, Seo K-W, Scheuchl B, Schrama EJO, Schröder L, Simonsen SB, Slater T, Spada G, Sutterley TC, Vishwakarma BD, van Wessem JM, Wiese D, van der Wal W, Wouters B (2023) Mass balance of the Greenland and Antarctic ice sheets from 1992 to 2020. *Earth Syst Sci Data* 15:1597–1616. <https://doi.org/10.5194/essd-15-1597-2023>
- Otosaka I, Shepherd A, Groh A (2021) Changes in Northwest Greenland Ice Sheet Elevation and Mass. EGU General Assembly 2021. <https://doi.org/10.5194/egusphere-egu21-2480>
- Palm SP, Yang Y, Spinhirne JD, Marshak A (2011) Satellite remote sensing of blowing snow properties over Antarctica. *J Geophys Res Atmosp*. <https://doi.org/10.1029/2011JD015828>
- Paolo FS, Fricker HA, Padman L (2015) Volume loss from Antarctic ice shelves is accelerating. *Science* 348:327–331. <https://doi.org/10.1126/science.aaa0940>
- Park JW, Gourmelen N, Shepherd A, Kim SW, Vaughan DG, Wingham DJ (2013) Sustained retreat of the Pine Island Glacier. *Geophys Res Lett* 40:2137–2142. <https://doi.org/10.1002/grl.50379>
- Pattyn F (2010) Antarctic subglacial conditions inferred from a hybrid ice sheet/ice stream model. *Earth Planet Sci Lett* 295:451–461. <https://doi.org/10.1016/j.epsl.2010.04.025>
- Pattyn F, Perichon L, Aschwanden A, Breuer B, de Smedt B, Gagliardini O, Gudmundsson GH, Hindmarsh RCA, Hubbard A, Johnson JV, Kleiner T, Kononov Y, Martin C, Payne AJ, Pollard D, Price S, Rückamp M, Saito F, Souček O, Sugiyama S, Zwinger T (2008) Benchmark experiments for higher-order and full-Stokes ice sheet models (ISMIP–HOM). *Cryosphere* 2:95–108. <https://doi.org/10.5194/tc-2-95-2008>
- Pattyn F, Schoof C, Perichon L, Hindmarsh RCA, Bueler E, de Fleurian B, Durand G, Gagliardini O, Gladstone R, Goldberg D, Gudmundsson GH, Huybrechts P, Lee V, Nick FM, Payne AJ, Pollard D, Rybak O, Saito F, Vieli A (2012) Results of the Marine Ice Sheet Model Intercomparison Project, MISIMP. *Cryosphere* 6:573–588. <https://doi.org/10.5194/tc-6-573-2012>
- Pattyn F, Favier L, Sun S, Durand G (2017) Progress in numerical modeling of Antarctic ice-sheet dynamics. *Curr Clim Change Rep* 3:174–184. <https://doi.org/10.1007/s40641-017-0069-7>
- Payne AJ, Nowicki S, Abe-Ouchi A, Agosta C, Alexander P, Albrecht T, Asay-Davis X, Aschwanden A, Barthel A, Bracegirdle TJ, Calov R, Chambers C, Choi Y, Cullather R, Cuzzone J, Dumas C, Edwards TL, Felikson D, Fettweis X, Galton-Fenzi BK, Goelzer H, Gladstone R, Golledge NR, Gregory JM, Greve R, Hattermann T, Hoffman MJ, Humbert A, Huybrechts P, Jourdain NC, Kleiner T, Munneke PK, Larour E, Le clec’h S, Lee V, Leguy G, Lipscomb WH, Little CM, Lowry DP, Morlighem M, Nias I, Pattyn F, Pelle T, Price SF, Quiquet A, Reese R, Rückamp M, Schlegel N-J, Seroussi H, Shepherd A, Simon E, Slater D, Smith RS, Straneo F, Sun S, Tarasov L, Trusel LD, Van Breedam J, van

- de Wal R, van den Broeke M, Winkelmann R, Zhao C, Zhang T, Zwinger T (2021) Future sea level change under coupled model intercomparison project phase 5 and phase 6 scenarios from the Greenland and Antarctic Ice Sheets. *Geophys Res Lett* 48:e2020GL091741. <https://doi.org/10.1029/2020GL091741>
- Peltier WR (2004) Global glacial isostasy and the surface of the ice-age earth: the ICE-5G (VM2) model and GRACE. *Annu Rev Earth Planet Sci* 32:111–149. <https://doi.org/10.1146/annurev.earth.32.082503.144359>
- Pritchard HD, Arthern RJ, Vaughan DG, Edwards LA (2009) Extensive dynamic thinning on the margins of the Greenland and Antarctic ice sheets. *Nature* 461:971–975. <https://doi.org/10.1038/nature08471>
- Rémy F, Flament T, Michel A, Verron J (2014) Ice sheet survey over Antarctica using satellite altimetry: ERS-2, Envisat, SARAL/AltiKa, the key importance of continuous observations along the same repeat orbit. *Int J Remote Sens* 35:5497–5512. <https://doi.org/10.1080/01431161.2014.926419>
- Rémy F, Flament T, Michel A, Blumstein D (2015) Envisat and SARAL/AltiKa observations of the Antarctic Ice Sheet: A comparison between the Ku-band and Ka-band. *Mar Geodesy* 38:510–521. <https://doi.org/10.1080/01490419.2014.985347>
- Ridley JK, Partington K (1988) A model of satellite radar altimeter return from ice sheets. *Remote Sens* 9:601–624. <https://doi.org/10.1080/01431168808954881>
- Rignot E (1996) Tidal motion, ice velocity and melt rate of Petermann Gletscher, Greenland, measured from radar interferometry. *J Glaciol* 42:476–485. <https://doi.org/10.3189/S002214300003464>
- Rignot E (2008) Changes in West Antarctic ice stream dynamics observed with ALOS PALSAR data. *Geophys Res Lett* 35:L12505. <https://doi.org/10.1029/2008GL033365>
- Rignot E, Casassa G, Gogineni P, Krabill W, Rivera A, Thomas R (2004) Accelerated ice discharge from the Antarctic Peninsula following the collapse of Larsen B ice shelf. *Geophys Res Lett* 31:L18401. <https://doi.org/10.1029/2004GL020697>
- Rignot E, Mouginot J, Scheuchl B (2011a) Antarctic grounding line mapping from differential satellite radar interferometry. *Geophys Res Lett.* <https://doi.org/10.1029/2011GL047109>
- Rignot E, Mouginot J, Scheuchl B (2011b) MEASURES InSAR-based Antarctica Ice velocity map NASA DAAC at the national snow and ice data center. Boulder Colorado. <https://doi.org/10.5067/MEASURES/CRYOSPHERE/nsidc-0484.001>
- Rignot E, Mouginot J, Morlighem M, Seroussi H, Scheuchl B (2014) Widespread, rapid grounding line retreat of Pine Island, Thwaites, Smith, and Kohler glaciers, West Antarctica, from 1992 to 2011. *Geophys Res Lett* 41:3502–3509. <https://doi.org/10.1002/2014GL060140>
- Rignot E, Mouginot J, Scheuchl B, van den Broeke M, van Wessem MJ, Morlighem M (2019) Four decades of Antarctic Ice Sheet mass balance from 1979–2017. *Proc Natl Acad Sci USA* 116:1095–1103. <https://doi.org/10.1073/pnas.1812883116>
- Ritz C, Edwards TL, Durand G, Payne AJ, Peyaud V, Hindmarsh RCA (2015) Potential sea-level rise from Antarctic ice-sheet instability constrained by observations. *Nature* 528:115–118. <https://doi.org/10.1038/nature16147>
- Roemer S, Legréy B, Horwath M, Dietrich R (2007) Refined analysis of radar altimetry data applied to the region of the subglacial Lake Vostok/Antarctica. *Remote Sens Environ* 106:269–284. <https://doi.org/10.1016/j.rse.2006.02.026>
- Sasgen I, Konrad H, Helm V, Grosfeld K (2019) High-resolution mass trends of the Antarctic ice sheet through a spectral combination of Satellite Gravimetry and Radar Altimetry Observations. *Remote Sens.* <https://doi.org/10.3390/rs11020144>
- Save H, Bettadpur S, Tapley BD (2016) High-resolution CSR GRACE RL05 mascons. *J Geophys Res Solid Earth* 121:7547–7569
- Scambos TA, Bohlander JA, Shuman CA, Skvarca P (2004) Glacier acceleration and thinning after ice shelf collapse in the Larsen B embayment Antarctica. *Geophys Res Lett.* <https://doi.org/10.1029/2004GL020670>
- Scheinert M, Engels O, Schrama EJ, van der Wal W, Horwath M (2023) Geodetic observations for constraining mantle processes in Antarctica. *Geol Soc London Memoirs* 56(1):295–313. <https://doi.org/10.1144/M56-2021-22>
- Schmidtke S, Heywood KJ, Thompson AF, Aoki S (2014) Multidecadal warming of Antarctic waters. *Science* 346:1227–1231. <https://doi.org/10.1126/science.1256117>
- Schoof C (2007) Ice sheet grounding line dynamics: steady states, stability, and hysteresis. *J Geophys Res Earth Surface.* <https://doi.org/10.1029/2006JF000664>
- Schröder L, Horwath M, Dietrich R, Helm V, van den Broeke MR, Ligtenberg SRM (2019) Four decades of Antarctic surface elevation changes from multi-mission satellite altimetry. *Cryosphere* 13:427–449. <https://doi.org/10.5194/tc-11-1111-2017>

- Seroussi H, Nakayama Y, Larour E, Menemenlis D, Morlighem M, Rignot E, Khazendar A (2017) Continued retreat of Thwaites Glacier, West Antarctica, controlled by bed topography and ocean circulation. *Geophys Res Lett* 44:6191–6199. <https://doi.org/10.1002/2017GL072910>
- Seroussi H, Nowicki S, Payne AJ, Goelzer H, Lipscomb WH, Abe-Ouchi A, Agosta C, Albrecht T, Asay-Davis X, Barthel A, Calov R, Cullather R, Dumas C, Galton-Fenzi BK, Gladstone R, Gollgede NR, Gregory JM, Greve R, Hattermann T, Hoffman MJ, Humbert A, Huybrechts P, Jourdain NC, Kleiner T, Larour E, Leguy GR, Lowry DP, Little CM, Morlighem M, Pattyn F, Pelle T, Price SF, Quiquet A, Reese R, Schlegel NJ, Shepherd A, Simon E, Smith RS, Straneo F, Sun S, Trusel LD, Van Breedam J, van de Wal RSW, Winkelmann R, Zhao C, Zhang T, Zwinger T (2020) ISMIP6 Antarctica: a multi-model ensemble of the Antarctic ice sheet evolution over the 21st century. *Cryosphere* 14:3033–3070. <https://doi.org/10.5194/tc-14-3033-2020>
- Shapiro NM, Ritzwoller MH (2004) Inferring surface heat flux distributions guided by a global seismic model: particular application to Antarctica. *Earth Planet Sci Lett* 223:213–224. <https://doi.org/10.1016/j.epsl.2004.04.011>
- Shepherd A, Ivins ER, Barletta GAVR, Bentley MJ, Bettadpur S, Briggs KH, Bromwich DH, Forsberg R, Galin N, Horwath M, Jacobs S, Joughin I, King MA, Jan TML, Li J, Stefan RML, Luckman A, Luthcke SB, McMillan M, Meister R, Milne G, Mouginot J, Muir A, Nicolas JP, Paden J, Payne AJ, Pritchard H, Rignot E, Rott H, Sørensen LS, Scambos TA, Scheuchl B, Ernst JOS, Smith B, Sundal AV, Jan HVA, Willem JVDB, Michiel RVDB, Vaughan DG, Velicogna I, Wahr J, Whitehouse PL, Wingham DJ, Yi D, Young D, Zwally HJ (2012) A reconciled estimate of Ice-Sheet mass balance. *Sci* 338(6111):1183–1189. <https://doi.org/10.1126/science.1228102>
- Shepherd A, Nowicki S (2017) Improvements in ice-sheet sea-level projections. *Nat Clim Chang* 7:672–674. <https://doi.org/10.1038/nclimate3400>
- Shepherd A, Wingham DJ, Mansley JAD (2002) Inland thinning of the Amundsen Sea sector, West Antarctica. *Geophys Res Lett* 29:1362–1364. <https://doi.org/10.1126/science.291.5505.862>
- Shepherd A, Ivins E, Rignot E, Smith B, van den Broeke M, Velicogna I, Whitehouse P, Briggs K, Joughin I, Krinner G, Nowicki S, Payne T, Scambos T, Schlegel N, Agosta C, Ahlstrøm A, Babonis G, Barletta V, Blazquez A, Bonin J, Csatho B, Cullather R, Felikson D, Fettweis X, Forsberg R, Gallee H, Gardner A, Gilbert L, Groh A, Gunter B, Hanna E, Harig C, Helm V, Horwath A, Horwath M, Khan S, Kjeldsen KK, Konrad H, Langen PL, Lecavalier B, Loomis B, Luthcke S, McMillan M, Melini D, Mernild S, Mohajerani Y, Moore P, Mouginot J, Moyano G, Muir A, Nagler T, Nield G, Nilsson J, Noel B, Ootaka I, Pattle ME, Peltier WR, Pie N, Rietbroek R, Rott H, Sandberg-Sørensen L, Sasgen I, Save H, Scheuchl B, Schrama E, Schröder L, Seo K-W, Simonsen S, Slater T, Spada G, Sutterley T, Talpe M, Tarasov L, van de Berg WJ, van der Wal W, van Wessem M, Vishwakarma BD, Wiese D, Wouters B (2018) Mass balance of the Antarctic Ice Sheet from 1992 to 2017. *Nature* 558:219–222. <https://doi.org/10.1038/s41586-018-0179-y>
- Shepherd A, Gilbert L, Muir AS, Konrad H, McMillan M, Slater T, Briggs KH, Sundal AV, Hogg AE, Engdahl M (2019) Trends in Antarctic ice sheet elevation and mass. *Geophys Res Lett* 46:8174–8183. <https://doi.org/10.1029/2019GL082182>
- Shepherd A, Ivins E, Rignot E, Smith B, van den Broeke M, Velicogna I, Whitehouse P, Briggs K, Joughin I, Krinner G, Nowicki S, Payne T, Scambos T, Schlegel N, Agosta C, Ahlstrøm A, Babonis G, Barletta VR, Bjørk AA, Blazquez A, Bonin J, Colgan W, Csatho B, Cullather R, Engdahl ME, Felikson D, Fettweis X, Forsberg R, Hogg AE, Gallee H, Gardner A, Gilbert L, Gourmelen N, Groh A, Gunter B, Hanna E, Harig C, Helm V, Horwath A, Horwath M, Khan S, Kjeldsen KK, Konrad H, Langen PL, Lecavalier B, Loomis B, Luthcke S, McMillan M, Melini D, Mernild S, Mohajerani Y, Moore P, Mottram R, Mouginot J, Moyano G, Muir A, Nagler T, Nield G, Nilsson J, Noël B, Ootaka I, Pattle ME, Peltier WR, Pie N, Rietbroek R, Rott H, Sandberg-Sørensen L, Sasgen I, Save H, Scheuchl B, Schrama E, Schröder L, Seo K-W, Simonsen SB, Slater T, Spada G, Sutterley T, Talpe M, Tarasov L, van de Berg WJ, van der Wal W, van Wessem M, Vishwakarma BD, Wiese D, Wilton D, Wagner T, Wouters B, Wuite J (2020) Mass balance of the Greenland Ice Sheet from 1992 to 2018. *Nature* 579:233–239. <https://doi.org/10.1038/s41586-019-1855-2>
- Simonsen SB, Sørensen LS (2017) Implications of changing scattering properties on Greenland ice sheet volume change from Cryosat-2 altimetry. *Remote Sens Environ* 190:207–216. <https://doi.org/10.1016/j.rse.2016.12.012>
- Simonsen SB, Stenseng L, Adalgeirsdóttir G, Fausto RS, Hvidberg CS, Lucas-Picher P (2013) Assessing a multilayered dynamic firm-compaction model for Greenland with ASIRAS radar measurements. *J Glaciol* 59:545–558. <https://doi.org/10.3189/2013JoG12I158>
- Simonsen SB, Barletta VR, Colgan WT, Sørensen LS (2021) Greenland ice sheet mass balance (1992–2020) from calibrated radar altimetry. *Geophys Res Lett* 48:e2020GL091216. <https://doi.org/10.1029/2020GL091216>

- Slater T, Shepherd A, McMillan M, Armitage TWK, Otosaka I, Arthern RJ (2019) Compensating changes in the penetration depth of pulse-limited radar altimetry over the Greenland ice sheet. *IEEE Trans Geosci Remote Sens* 57:9633–9642. <https://doi.org/10.1109/TGRS.2019.2928232>
- Slater T, Hogg AE, Mottram R (2020) Ice-sheet losses track high-end sea-level rise projections. *Nat Clim Chang* 10:879–881. <https://doi.org/10.1038/s41558-020-0893-y>
- Smith B, Fricker HA, Gardner AS, Medley B, Nilsson J, Paolo FS, Holschuh N, Adusumilli S, Brunt K, Csatho B, Harbeck K, Markus T, Neumann T, Siegfried MR, Zwally HJ (2020) Pervasive ice sheet mass loss reflects competing ocean and atmosphere processes. *Science* 368:1239–1242. <https://doi.org/10.1126/science.aaz5845>
- Smith BE, Medley B, Fettweis X, Sutterley T, Alexander P, Porter D, Tedesco M (2022) Evaluating Greenland surface-mass-balance and firn-densification data using ICESat-2 altimetry. *Cryosp Discuss* 1:24. <https://doi.org/10.5194/tc-2022-44>
- Stibal M, Box JE, Cameron KA, Langen PL, Yallop ML, Mottram RH, Khan AL, Molotch NP, Christmas NAM, Cali Quaglia F, Remias D, Smeets CJPP, van den Broeke MR, Ryan JC, Hubbard A, Tranter M, van As D, Ahlström AP (2017) Algae DRIVE ENHANCED DARKENING OF BARE Ice on the Greenland Ice Sheet. *Geophys Res Lett* 44(11):463–511. <https://doi.org/10.1002/2017GL075958>
- Sun Y, Riva R, Ditmar P (2016) Optimizing estimates of annual variations and trends in geocenter motion and J2 from a combination of GRACE data and geophysical models. *J Geophys Res Solid Earth* 121:8352–8370. <https://doi.org/10.1002/2016JB013073>
- Sundal AV, Shepherd A, Nienow P, Hanna E, Palmer S, Huybrechts P (2011) Melt-induced speed-up of Greenland ice sheet offset by efficient subglacial drainage. *Nature* 469:522–U583. <https://doi.org/10.1038/nature09740>
- Swenson S, Wahr J (2002) Methods for inferring regional surface-mass anomalies from Gravity Recovery and Climate Experiment (GRACE) measurements of time-variable gravity. *J Geophys Res Solid Earth* 107(B9):ETG-3. <https://doi.org/10.1029/2001JB000576>
- Swenson S, Wahr J (2006) Post-processing removal of correlated errors in GRACE data. *Geophys Res Lett*. <https://doi.org/10.1029/2005GL025285>
- Tapley BD, Watkins MM, Flechtner F, Reigber C, Bettadpur S, Rodell M, Sasgen I, Famiglietti JS, Landerer FW, Chambers DP, Reager JT, Gardner AS, Save H, Ivins ER, Swenson SC, Boening C, Dahle C, Wiese DN, Dolslaw H, Tamisiea ME, Velicogna I (2019) Contributions of GRACE to understanding climate change. *Nat Clim Chang* 5:358–369. <https://doi.org/10.1038/s41558-019-0456-2>
- Turner J, Lu H, White I, King JC, Phillips T, Hosking JS, Bracegirdle TJ, Marshall GJ, Mulvaney R, Deb P (2016) Absence of 21st century warming on Antarctic Peninsula consistent with natural variability. *Nature* 535:411–415. <https://doi.org/10.1038/nature18645>
- van As D, Fausto RS, PROMICE project team, (2011) Programme for monitoring of the Greenland Ice Sheet (PROMICE): first temperature and ablation records. *GEUS Bull* 23:73–76. <https://doi.org/10.34194/geusb.v23.4876>
- van Wessem JM, van de Berg WJ, Noël BPY, van Meijgaard E, Amory C, Birnbaum G, Jakobs CL, Krüger K, Lenaerts JTM, Lhermitte S, Ligtenberg SRM, Medley B, Reijmer CH, van Tricht K, Trusel LD, van Ulfth LH, Wouters B, Wuite J, van den Broeke MR (2018) Modelling the climate and surface mass balance of polar ice sheets using RACMO2—Part 2: Antarctica (1979–2016). *Cryosphere* 12:1479–1498. <https://doi.org/10.5194/tc-12-1479-2018>
- Vandecrux B, MacFerrin M, Machguth H, Colgan WT, van As D, Heilig A, Stevens CM, Charalampidis C, Fausto RS, Morris EM, Mosley-Thompson E, Koenig L, Montgomery LN, Miège C, Simonsen SB, Ingeman-Nielsen T, Box JE (2019) Firn data compilation reveals widespread decrease of firn air content in western Greenland. *Cryosphere* 13:845–859. <https://doi.org/10.5194/tc-13-845-2019>
- Vaughan DG, Marshall GJ, Connolley WM et al (2003) Recent rapid regional climate warming on the antarctic peninsula. *Clima Chang* 60:243–274. <https://doi.org/10.1023/A:1026021217991>
- Velicogna I, Wahr J (2013) Time-variable gravity observations of ice sheet mass balance: precision and limitations of the GRACE satellite data. *Geophys Res Lett* 40:3055–3063. <https://doi.org/10.1002/grl.50527>
- Velicogna I, Mohajerani Y, Geruo A, Landerer F, Mougnot J, Noel B, Rignot E, Sutterley T, van den Broeke M, van Wessem JM, Wiese D (2020) Continuity of ice sheet mass loss in Greenland and Antarctica from the GRACE and GRACE Follow-Onmissions. *Geophys Res Lett* 47:e2020GL087291. <https://doi.org/10.1029/2020gl087291>
- Verjans V, Leeson AA, McMillan M, Stevens CM, van Wessem JM, van de Berg WJ, van den Broeke MR, Kittel C, Amory C, Fettweis X, Hansen N, Bøberg F, Mottram R (2021) Uncertainty in East Antarctic firn thickness constrained using a model ensemble approach. *Geophys Res Lett* 48:e2020GL092060. <https://doi.org/10.1029/2020GL092060>

- Wahr J, Molenaar M, Bryan F (1998) Time variability of the Earth's gravity field: Hydrological and oceanic effects and their possible detection using GRACE. *J Geophys Res Solid Earth* 103:30205–30229. <https://doi.org/10.1029/98JB02844>
- Watkins MM, Wiese DN, Yuan D-N, Boening C, Landerer FW (2015) Improved methods for observing Earth's time variable mass distribution with GRACE using spherical cap mascons. *J Geophys Res Solid Earth* 120:2648–2671
- Werder MA, Hewitt IJ, Schoof CG, Flowers GE (2013) Modeling channelized and distributed subglacial drainage in two dimensions. *J Geophys Res Earth Surf* 118:2140–2158. <https://doi.org/10.1002/jgrf.20146>
- Whitehouse PL (2018) Glacial isostatic adjustment modelling: historical perspectives, recent advances, and future directions. *Earth Surf Dyn* 6:401–429. <https://doi.org/10.5194/esurf-6-401-2018>
- Whitehouse PL, Gomez N, King MA, Wiens DA (2019) Solid earth change and the evolution of the Antarctic Ice Sheet. *Nat Commun*. <https://doi.org/10.1038/s41467-018-08068-y>
- Willen MO, Horwath M, Schröder L, Groh A, Ligtenberg SRM, Kuipers Munneke P, van den Broeke MR (2020) Sensitivity of inverse glacial isostatic adjustment estimates over Antarctica. *Cryosphere* 14:349–366. <https://doi.org/10.5194/tc-14-349-2020>
- Willen MO, Broerse T, Groh A, Wouters B, Kuipers Munneke P, Horwath M, van den Broeke MR, Schröder L (2021) Separating long-term and short-term mass changes of Antarctic Ice drainage basins: a coupled state space analysis of satellite observations and model products. *J Geophys Res Earth Surf*. <https://doi.org/10.1029/2020JF005966>
- Willen MO, Horwath M, Groh A, Helm V, Uebbing B, Kusche J (2022) Feasibility of a global inversion for spatially resolved glacial isostatic adjustment and ice sheet mass changes proven in simulation experiments. *J Geodesy* 96(10):75. <https://doi.org/10.1007/s00190-022-01651-8>
- Wilson N, Straneo F, Heimbach P (2017) Satellite-derived submarine melt rates and mass balance (2011–2015) for Greenland's largest remaining ice tongues. *Cryosphere* 11:2773–2782. <https://doi.org/10.5194/tc-11-2773-2017>
- Wingham DJ, Ridout AJ, Scharroo R, Arthern RJ, Shum CK (1998) Antarctic Elevation Change from 1992 to 1996. *Science* 282:456–458. <https://doi.org/10.1126/science.282.5388.456>
- Wouters B, Bonin JA, Chambers DP, Riva REM, Sasgen I, Wahr J (2014) GRACE, time-varying gravity, Earth system dynamics and climate change. *Rep Prog Phys* 77:116801. <https://doi.org/10.1088/0034-4885/77/11/116801>
- Young TJ, Christoffersen P, Bougamont M, Tulaczyk SM, Hubbard B, Mankoff KD, Nicholls KW, Stewart CL (2022) Rapid basal melting of the Greenland Ice Sheet from surface meltwater drainage. *Proc Natl Acad Sci* 119:2116036119. <https://doi.org/10.1073/pnas.2116036119>
- Yuan DN (2018) JPL level-2 processing standards document for level-2 product release 06 (Rev. 6.0, June 1). GRACE Publication, pp 327–744
- Zwally HJ, Bindshadler RA, Brenner AC, Major JA, Marsh JG (1989) Growth of Greenland Ice Sheet: measurement. *Science* 246:1587–1589. <https://doi.org/10.1126/science.246.4937.1587>

Publisher's Note Springer Nature remains neutral with regard to jurisdictional claims in published maps and institutional affiliations.